AD-786 560

STRUCTURAL EVALUATION OF UH-1D TUBULAR ROTOR BLADE

Don Cook

Fiber Science, Incorporated

Prepared for:

Army Air Mobility Research and Development Laboratory

August 1974

EUSTIS DIRECTORATE POSITION STATEMENT

The report has been reviewed by the Eustis Directorate, U. S. Army Air Mobility Research and Development Laboratory and is considered to be technically sound.

This program was conducted under the technical management of Mr. I. E. Figge, Technology Applications Division.

DISCLAIMERS

The findings in this report are not to be construed as an official Department of the Army position unless so designated by other authorized documents.

When Government drawings, specifications, or other data are used for any purpose other than in connection with a definitely related Government procurement operation, the United States Government thereby incurs no responsibility nor any obligation whatsoever; and the fact that the Government may have formulated, furnished, or in any way supplied the said drawings, specifications, or other data is not to be regarded by implication or otherwise as in any manner licensing the holder or any other person or corporation, or conveying any rights or permission, to manufacture, use, or sell any patented invention that may in any way be related thereto.

Trade names cited in this report do not constitute an official endorsement or approval of the use of such commercial hardware or software.

DISPOSITION INSTRUCTIONS

Destroy this report when no longer needed. Do not return it to the originator.

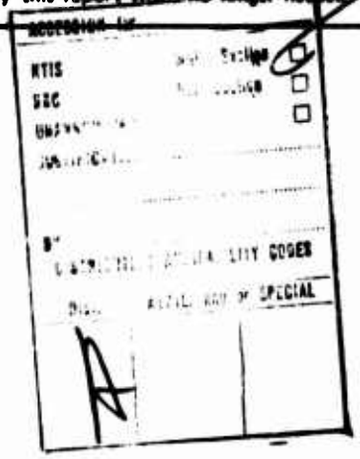

Unclassified

SECURITY CLASSIFICATION OF THIS PAGE (When Data Entered)

REPORT DOCUMENTATION PAGE		READ INSTRUCTIONS BEFORE COMPLETING FORM
1. REPORT NUMBER USAAMRDL-TR-74-41	2. GOVT ACCESSION NO.	3. RECIPIENT'S CATALOG NUMBER AD-786 560
4. TITLE (and Subtitle) STRUCTURAL EVALUATION OF UH-1D TUBULAR ROTOR BLADE		5. TYPE OF REPORT & PERIOD COVERED Final
		6. PERFORMING ORG. REPORT NUMBER
7. AUTHOR(s) Don Cook		8. CONTRACT OR GRANT NUMBER(s) DAAJ02-73-C-0042
9. PERFORMING ORGANIZATION NAME AND ADDRESS Fiber Science, Inc. Gardena, California 90248		10. PROGRAM ELEMENT, PROJECT, TASK AREA & WORK UNIT NUMBERS Task 1F162208A17003
11. CONTROLLING OFFICE NAME AND ADDRESS Eustis Directorate U. S Army Air Mobility Research and Development Laboratory, Fort Eustis, Va.		12. REPORT DATE August 1974 13. NUMBER OF PAGES 55
14. MONITORING AGENCY NAME & ADDRESS(if different from Controlling Office)		15. SECURITY CLASS. (of this report) Unclassified 15a. DECLASSIFICATION/DOWNGRADING SCHEDULE

16. DISTRIBUTION STATEMENT (of this Report)

Approved for public release; distribution unlimited.

17. DISTRIBUTION STATEMENT (of the abstract entered in Block 20, if different from Report)

18. SUPPLEMENTARY NOTES

19. KEY WORDS (Continue on reverse side if necessary and identify by block number)

Helicopters
Rotor Blades(Rotary Wings)
Filament Wound Construction
Destructive Tests
Non destructive Testing
Repair
Rotor Blades

20. ABSTRACT (Continue on reverse side if necessary and identify by block number)

The purpose of this evaluation was to determine the effects of static loading, cyclic loading and ballistic damage/repairs on the stiffness and resonant behavior of three full-scale, filament-wound tubular-reinforced UH-1D main rotor blades (S/N 001, S/N 002, and S/N 003) previously fabricated under Contract DAAJ02-72-C-013. Blades S/N 001 and S/N 002 were made predominately from glass Fibers. Blade S/N 003 included the use of Kevlar 49 as the skin fiber. All three blades were subjected to static deflection, dynamic, proof, creep, fatigue, and ultimate testing. In addition, blades

DD FORM 1 JAN 73 1473 EDITION OF 1 NOV 65 IS OBSOLETE

Unclassified

SECURITY CLASSIFICATION OF THIS PAGE (When Data Entered)

S/N 002 and S/N 003 were subjected to ballistic impact, ball drop, and simulated tree strike testing.

There were no deleterious effects from the static proof tests except for damage sustained by blade S/N 001 during an excessively high chordwise loading. The uncommonly high and erroneous loading was applied at the tip, placing the trailing edge of the blade in compression. At 1650 pounds the trailing edge separated, resulting in an opening approximately 57 inches long (spanwise) and with a maximum depth of 15 inches at a point approximately 55 inches from the root end. The damage was easily repaired, and from all indications the blade was restored to its original condition.

Blades S/N 001 and S/N 002 sustained damage to their root ends during fatigue testing. This was attributed to:

(1) Fit of main attachment pin was loose.
(2) Test fixture did not clamp sides of root end as in actual use.
(3) Specified test level was too high.

All three blades were tested flapwise to ultimate after completion of fatigue testing. S/N 001 sustained damage sufficient to stop the test at approximately 3.38 times limit load; S/N 002 test terminated at 4.12 times limit load; and S/N 003 was damaged at 3.55 times limit load. Damage in S/N 001 and S/N 002 began in the root end areas previously damaged during fatigue testing. S/N 003 sustained compression failure of the skin at Station 84 with some splitting of the leading edge. The lower compression strength of S/N 003 should be anticipated in view of Kevlar-49 fiber in the skin. The blades were not tested to complete ultimate failure due to the considerable and unexpected deflection that would have been necessary. None of the damage completely disabled the blades and they were still considered to be structurally intact.

Damage from bullet impact was not considered excessive, and the effects of the ball drop and tree impacts were surprisingly minor. In the case of the tree impact tests, there was no damage at all.

PREFACE

The testing program described herein was performed under Contract DAAJ02-73-C-0042 (DA Task 1F162208A17003) for the Eustis Directorate, U. S. Army Air Mobility Research and Development Laboratory, Fort Eustis, Virginia. Mr. I. E. Figge was the Army program director.

TABLE OF CONTENTS

LIST OF ILLUSTRATIONS

LIST OF TABLES

INTRODUCTION

The three filament-wound tubular-reinforced UH-1D helicopter main rotor blades tested under this program were designed, fabricated and received limited testing under Contract DAAJ02-72-C-0013 as reported in USAAMRDL Technical Report 73-61.* The original program was highly successful in that a new and unique rotor blade design was successfully demonstrated having the following potential advantages over existing metal blades:

1. Longer life (better fatigue strength).
2. Lower cost.
3. Easier to repair damaged areas.
4. Higher ballistic tolerance.
5. Lower radar profile.
6. Redundant load paths.
7. Higher strength.
8. Higher reliability.
9. Higher resistance to handling damage.
10. Lower tooling cost.
11. Automatic machine fabrication.

Three blades were fabricated nearly identical to each other except that one, S/N003, was constructed using Kevlar-49 fibers as skin material instead of glass fibers as in the other two blades. The blades were 24 feet long from the center of rotation to the tip with a chord length of 21 inches and a basic NACA-0012 airfoil shape except in the root-end fitting area.

As a result of the successful completion of the initial program it became apparent that much more could be learned of the full structural potential of this highly promising blade design. An extensive test program was developed to measure the effect of static bending (proof) and dynamic loads, bullet impact and bullet impact damage repair on the creep (static deflection), stiffness and dynamic response. Also to be measured were the ultimate beamwise bending strength, the effect of a simulated tree strike and the maximum drop height of a 2-pound steel ball without causing any damage to the blade.

Additional static deflection and dynamic test methods were designed and implemented in the program to detect any changes in the basic structure of the blades resulting from the loadings described above. Test parameters were based on data accumulated in reports of the actual inflight loads of the currently operational metal blade.

The following sections in this report describe the loads, test methods, and test results operative in the test program. The test sequence of the operations on each blade is shown in Table 1.

---

* UH-1D FILAMENT-WOUND TUBULAR-REINFORCED ROTOR BLADE, USAAMRDL Technical Report 73-61, Eustis Directorate, U. S. Army Air Mobility Research and Development Laboratory, Fort Eustis, Virginia, October 1973.

TABLE 1 - TEST SEQUENCE

S/N 001

1. Static Deflection (Creep)
2. Dynamic
3. Proof (Flapwise and Chordwise)*
4. Static Deflection (Creep)
5. Dynamic
6. Repair of Chordwise Proof Test Failure
7. Static Deflection (Creep)
8. Dynamic
9. Fatigue
10. Static Deflection (Creep)
11. Dynamic
12. Ultimate

* Torsional proof test was performed after repair of blade (Sequence No. 6) and before Creep test No. 7.

S/N 002

1. Static Deflection (Creep)
2. Dynamic
3. Proof
4. Static Deflection (Creep)
5. Dynamic
6. Bullet Impact - Leading Edge
7. Static Deflection (Creep)
8. Dynamic
9. Repair - Ballistic Spar (Leading Edge) Damage
10. Static Deflection (Creep)
11. Dynamic
12. Bullet Impact - Trailing Edge
13. Static Deflection (Creep)
14. Dynamic
15. Repair - Ballistic Trailing Edge Damage
16. Static Deflection (Creep)
17. Dynamic
18. Fatigue
19. Dynamic
20. Static Deflection (Creep)
21. Ultimate
22. Ball Drop
23. Simulated Tree Strike

S/N 003

1. Static Deflection (Creep)
2. Dynamic
3. Proof
4. Static Deflection (Creep)
5. Dynamic
6. Fatigue
7. Static Deflection (Creep)
8. Dynamic
9. Ultimate
10. Simulated Tree Strike
11. Ball Drop
12. Ballistic Impact - Trailing and Leading Edge

BLADE PREPARATION

The blades were prepared for testing by installing reinforcement blocks between the skins in the root end area and a root end attachment plate on the root end. The attachment plate was secured to the root end using nine 5/8-inch-diameter rods that connected to the root end fitting and four bolts connected to two pins installed through the blade. The plate and pin installation can be seen in the figures describing the various tests. Holes for the pins were bored through the blades as shown in Figure 1. The nuts installed on the 5/8-inch rods were torqued to 37 ft-lb against the plate.

A tip end fixture was fabricated to facilitate the application of the loads at the blade tip. The fixture consisted of two 4-inch by 6-inch blocks of wood which were clamped to the tip of the blade with bolts at the leading and trailing edges. The blocks were contoured to the shape of the blade tip with a hard rubber liner installed to contact the blade. A steel plate with a shoulder bolt in the center was installed to connect the wood blocks across the face of the blade tip. The shoulder bolt was 5.0 inches from the leading edge and served as a trunnion to which all flapwise and chordwise loads were applied; it also acted as the pivot for the torsional loading tests.

TESTS

STATIC DEFLECTION AND CREEP TESTS

The static deflection tests consisted of securing the root end to a reaction mass and applying loads to the blade tip in flapwise, chordwise and torsional modes.

The reaction mass was a block of concrete 4 feet wide, 4 feet deep, and 4 feet from the floor. It also extended approximately 4 feet below the floor. A 2-inch-thick steel face plate was attached to a side and top surface of the mass using pipes that extended through the mass. The side face plate served as the attachment for the blade root end plate. The top plate attached two pillow blocks for the torsional tests.

Loads were applied at the tip end of the blade in the vertical direction using a 15-foot-high "A-Frame" structure on caster wheels. The wheels provided movement of the frame in any horizontal direction to keep the load directly over the tip. A hand-operated hoist was connected between the top of the "A-Frame" and the tip end fixture and operated to apply the loads to the tip. The load magnitude was determined using a load cell connected between the hoist and the fixture.

Three small gage blocks were bonded on the blades at Stations 88.0, 138.0, 188.0, 238.0 and 284.0. A block was located at each station on the leading edge, trailing edge, and over the spar (5 inches from the leading edge). Two beams were installed on the floor under the blades to provide a solid base and reference plane from which the measurements of the blade deflections could be made. The beams ran the entire length of the blades and were grouted and clamped to the floor. Measurements were made from the beams to the gage blocks using either a 48-inch height gage mounted on a base which spanned the beams or a 12-foot tape. A 24-inch machinist's scale was used to measure lateral motion of the blade. The height gage also provided a measurement reference plane normal to the plane formed by the beams.

Flapwise deflections were applied and measured with the blades mounted horizontally so that the chord at the root end was parallel to the floor beam reference plane. To establish a zero position, the tip was loaded until the blade was level at the mid section. Measurements were then made to each gage block and recorded on the data sheet under the no-load column. A 50-pound load was then applied and held, and measurements were taken again at the same points. Figures 2 and 3 are photographs of the typical flapwise test arrangement. The test arrangement for chordwise testing was the same as the flapwise position except the blade was rotated 90° so that the chord was normal to the floor beam reference plane with the trailing edge up (see Figures 4, 5, and 6). The loading applied in the chordwise direction was 250 pounds.

The torsional test blade position was the same as chordwise. Loading was accomplished by restraining the blade tip from flapwise and chordwise movement and applying a 400-lb load perpendicular to the chord 25 inches from the center of the tip fixture trunnion (10,000 in-lb moment). The rotation of the tip end was about the trunnion (see Figures 7 and 8). Figure 9 exemplifies the method of obtaining a typical measurement.

DYNAMIC TESTS

Dynamic testing consisted of driving the root end of the blade with an electrodynamic shaker to determine the first, second and third flapwise natural frequencies and mode shapes; the first chordwise natural frequency and mode shapes; and the first and second torsional natural frequencies and mode shapes.

Flapwise and chordwise testing was accomplished using the concrete mass described under static deflection tests. The blades were attached to the block for flapwise and chordwise testing with a flexure as shown in Figures 10 and 11. The torsional vibration was produced by attaching the root end of the blade to a tube which was installed in two pillow blocks on top of the reaction mass. A drive rod from the shaker armature attached to the root end plate in such a manner that when the shaker was operated the blade was vibrated torsionally. Figure 12 is a photograph of a typical torsional test arrangement.

Testing consisted of vibrating the blade sinusoidally and varying the frequency until the blade's natural frequencies were found. When a frequency was found, the double amplitude of the trailing edge was measured at Stations 88.0, 138.0, 188.0, 238.0 and 288.0 and the root end.

PROOF TESTS

Proof testing was conducted to determine if the blades could withstand 150% design loads when loaded in the flapwise, chordwise and torsional modes. The test setup and manner of loading were in the same manner as the static deflection test. Figures 13 through 18 are photographs of typical proof test arrangements.

The 150% design loads applied to the blades' tips were as follows:

	S/N001	S/N002	S/N003
Flapwise	333 lb	333 lb	333 lb
Chordwise	1650 lb	1145 lb	1145 lb
Torsional	1875 ft-lb	1875 ft-lb	1875 ft-lb

During the chordwise portion of the test on S/N001, the blade failed at a loading of 1650 pounds. The flapwise proof loading was previously done and the torsional proof was to follow. Because of the failure the torsional test was postponed, and the blade was submitted to static deflection and dynamic testing in the damaged condition. The blade was then repaired and the torsional proof test was completed. As a result of this breakage, the chord and torsional proof loading test requirements were reviewed and found to be excessive. They were subsequently reduced for the remaining tests on the other blades. There were no other proof test blade failures.

FATIGUE TESTS

Fatigue testing was performed to evaluate the ability of the blades to withstand 10^6 cycles of alternating stress at the maximum bending strains typical of what would be encountered in flight. Testing was done in the flapwise mode at the third flapwise natural frequency using the same test configuration as described for flapwise testing under the section entitled "Dynamic Testing". Two strain gages were installed on both sides of the blades at the point of maximum skin stress and blade half-thickness (6.5 inches from leading edge and approximately 90 inches from the root end) to establish the proper level of test strain.

During testing the frequency was continually checked and adjusted as necessary to maintain the vibration at the third natural frequency point. The strain gages usually failed in the first 30 minutes of testing. Test levels were maintained from then on by measuring the double amplitude displacement of the blade at the strain gage location (see Figure 19) and adjusting the shaker force applied at the root end to maintain the same displacement as recorded when the strain gages were in operation. Only minor adjustments were required.

All motion of the blade was measured by placing a machinist's scale adjacent to a portion of the blade such as the trailing edge, and observing the maximum points of deflection. Deflection of the blade could be easily seen and measured in this manner (see Figure 20).

The equivalent flight loads and estimated number of cycles at each load level are shown in Table 2. The maximum stress and strain levels in the blade skin at 6.5 inches aft of the leading edge calculated for the equivalent flight loads are shown in Table 3.

TABLE 2 - EQUIVALENT FLIGHT LOADS AT STATION 85.25 CONVERTED TO BEAMWISE BENDING

Condition	No. Cycles	M_b, in.-lb		M_b, *in.-lb
		Mean	Alternating	Equiv. R=-1
Steady	450,000	12,000	±10,000	10,833
Med. Maneuvers	350,000	20,000	±19,000	21,794
Max. Maneuvers	200,000	29,000	±28,000	34,393

* Based on Goodman diagram and an ultimate moment of 156,000 in.-lb (skin stress at failure assumed 26,000 psi).

$$M_b{}^* = \left\{ \frac{M_{alternating}}{1 - \frac{M_{mean}}{M_{ultimate}}} \right\}$$

TABLE 3 - CALCULATED SKIN STRESS AND STRAIN FOR EQUIVALENT FLIGHT LOADS AT BLADE STATION 85.25

	S/N 001	S/N 002	S/N 003
	psi	psi	
E_{skin}, 10^6 psi	1.834	1.834	2.975
EI_x, 10^6 lb-in.^{2}	13.86	15.27	20.79
Stress, psi		Stress, psi	
M_b = 10,833 in.-lb	1806	1639	1953
M_b = 21,794 in.-lb	3633	3298	3930
M_b = 34,393 in.-lb	5734	5204	6201
Strain, in./in.		Strain, in./in.	
M_b = 10,833 in.-lb	.000985	.000894	.000656
M_b = 21,794 in.-lb	.001981	.001798	.001321
M_b = 34,393 in.-lb	.003126	.002837	.002084

$$\sigma = \frac{M_b C E_{skin'}}{EI_x} \text{ psi}$$

$$\epsilon = \frac{M_b C}{EI_x}, \text{ in./in.}$$

C = 1.26 in.

The approximate bending moment at the root end of the blade is calculated as follows:

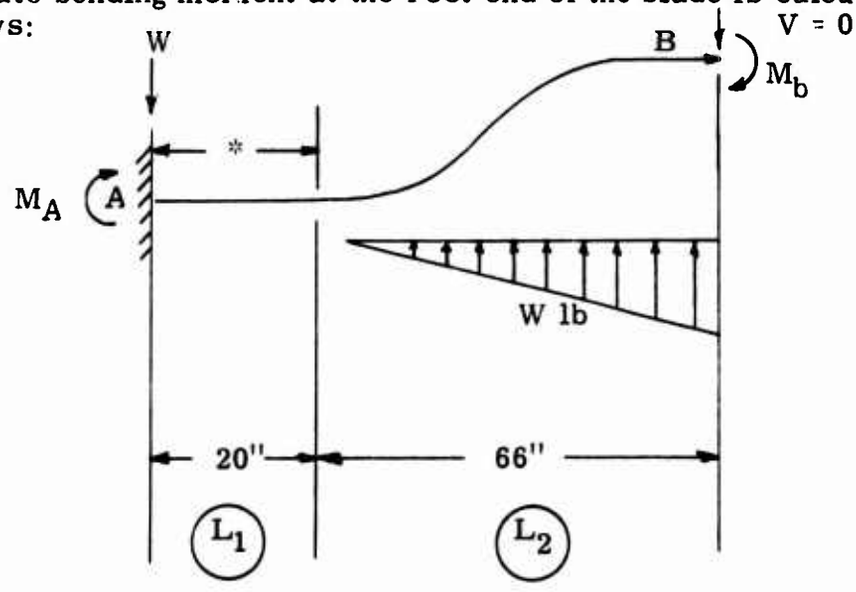

* Rotation assumed to be zero in this area because of the large stiffness increase relative to the remaining blade

Equal rotations at point B and solving for W

$$\frac{M_b L_2}{EI} = \frac{W L_2^2}{4 EI}$$

$$W = \frac{4 M_b}{L_2}$$

With W known the moment at the root end (point A) is

$$M_A = (L_1 + \frac{2}{3} L_2) W - M_b$$

M_b in. -lb	W lb	M_A in. -lb
10, 833	657	31, 185
21, 794	1320	62, 740
34, 393	2084	99, 010

The maximum design bending moment at the root end is 250, 000 in. -lb (single cycle loading).

ULTIMATE TESTS

Ultimate testing was performed to determine the point at which the blades would fail in bending flapwise. The methods of loading and restraining the blades were exactly the same as those described under the flapwise static deflection, creep and proof testing. The force applied to the tip was maintained directly over the trunnion by moving the "A-Frame" structure as required to keep the load vertical.

BALLISTIC (BULLET IMPACT) TESTS

Bullet impact tests were performed on Blades S/N 002 and S/N 003 to determine the extent of the damage when the blades are hit by .30 caliber ball ammunition on the leading and trailing edges at a velocity of 1800 feet per second. Bullet damage was repaired on Blade S/N 002 and not repaired on S/N 003.

The ammunition used was from Lot No. LC-12377 which was loaded at Lake City Arsenal in September 1943. The bullets were 30-06 AP, steel core copper clad, and weighed between 163 and 165 grains.

To obtain the proper velocity, several rounds were disassembled and reloaded with the same powder in varying amounts and fired through a chronograph to determine the amount of powder required to obtain an 1800-foot-per-second velocity. Thirty rounds were loaded with the reduced amount of powder (36 grains). Six of the 30 rounds were fired for velocity and all fell within a range of between 1775 and 1805 feet per second. Cartridges from the remaining 24 rounds were used to determine tumbling characteristics and for the actual test.

The test gun was a Mauser Action 8mm rechambered to accept the 30-06 cartridge. The muzzle was sawed off at approximately a 45° angle to the bore. Bullet tumbling from the test gun was determined by firing several rounds through paper targets located 2, 3, 4, 6, 8, 10, and 12 feet from the muzzle. The holes in the targets were measured to determine the bullet angle at penetration.

Requirements for the leading edge hit were that the bullet impact on its side, tangent to the leading edge surface with the line of flight at a 30° angle from the chord. Impact was specified at 1.0 inch from the leading edge. This required the bullet to pitch 48° from its line of flight (see Figure 22). To obtain the 48° pitch, the bullet was fired with the muzzle 3 feet 4 inches from the impact point.

Trailing edge requirements were nearly the same as the leading edge except the point of impact was 1.1 inches from the trailing edge. However, to obtain a tangential hit the bullet pitch angle required was 38° (see Figure 22). To obtain this, the muzzle of the test gun was placed 2 feet 10 inches from the point of impact.

The test arrangement (see Figure 23) consisted of boxing in the section of the blade to be tested and filling the area in the box around the blade with sand to stop the bullet after it hit the blade. A path for the bullet was made by inserting a pipe through a side of the box with the opening near the specified point of impact and the centerline of the pipe at an angle of 30° to the chord. The area around the impact point on the blade was kept clear of sand by a piece of sheet rubber that connected to the end of the pipe and the blade. The test gun was held, aimed, and fired manually after positioning for the proper angle and muzzle to impact point distance.

SIMULATED TREE STRIKE TESTS

The simulated tree strike test was performed to simulate the impact energy of the blade traveling at 324 rpm and striking a 3-inch-diameter tree. The kinetic energy of the impact was calculated to be 7207 ft/lb. This was simulated by dropping a 3-inch-diameter Douglas fir dowel, 15 inches long, suspended between two 360-pound weights, from a height of 10 feet onto the leading edge of the blade. The blade was supported with the chord vertical (leading edge up) by two chocks, one located at Station 250 and the other at Station 286, with the impact point at Station 268.

The weights consisted of two 55-gallon barrels with the tops removed. A steel pipe, approximately 3-1/4 inches inside diameter, was installed through the sides of the barrels to accommodate the fir dowel. The weights were connected by a truss mounted on top of the barrels with a bolt in the center to connect to a quick-release mechanism. Each barrel was brought to the proper weight of 360 pounds by adding sand.

The chocks with blade installed were positioned on a 2-inch-thick flat plate providing a solid base to react the energy from the impact.

The barrels were lifted 10 feet directly above the blade leading edge impact point using a forklift. A plumb bob was used to make the final determination of the drop point. The weights were released using a quick-disconnect mechanism from the forklift platform and allowed to free fall, impacting the dowel on the blade.

BALL DROP TESTS

Ball drop testing consisted of dropping a 2.0-pound spherical steel ball, 2.36 inches in diameter, from a height of 6 feet onto the surface of the blade. The blade was positioned such that the fall of the ball was perpendicular to the chord. Three impact areas were specified. The first was at Station 180 and 3.5 inches from the leading edge; the second was at Station 200 and 10.0 inches from the leading edge; and the third was at Station 220 and 19.5 inches from the leading edge. If no damage was incurred by the first drop (6 feet), other drops were made, increasing in 1-foot increments, until damage occurred. Testing was specified on Blades S/N 002 and S/N 003.

RESULTS

STATIC DEFLECTION AND CREEP TESTS

The flapwise, chordwise and torsional static deflection data is summarized in Tables 4, 5, and 6. Figures 24, 25 and 26 show graphically the measured deflection data plotted versus the test sequence number. The minor differences in the data from static deflection and creep tests are due largely to the inability to repeat the same test conditions from one test to the next.

There was a perceptible change in the blade stiffness resulting from the failure during chordwise proof testing of S/N 001 and leading and trailing edge bullet impact of S/N 002. Subsequent repairs restored the blades to their original conditions.

DYNAMIC TESTS

The flapwise, chordwise and torsional dynamic data is summarized in Tables 7, 8 and 9.

Figures 24, 25 and 26 present the natural frequencies along with the test sequence and static deflection data.

PROOF TESTS

The blades were subjected to 150% of limit flapwise and chordwise bending and torsional loads except for the chordwise loading portion on Blade S/N 001. During the chordwise portion of the test on S/N 001, the blade failed at a loading of 1650 pounds. When the 1650-pound load was reached, audible cracking noises were heard coming from the general area toward the root end third of the blade. Application of the loading was stopped and the blade was observed. More cracking was heard and the trailing edge around Station 50 became unstable and took a serpentine shape. This condition progressed for about 5 seconds and then the trailing edge separated suddenly with a loud bang. Separation occurred in the material near the bond line and also in the foam beginning at 27.5 inches from the root end and extending to 84.5 inches from the root end. The total length of the split was 57 inches. The foam separation depth varied from very little at both ends of the split to a maximum of 15 inches at a point approximately 55 inches from the root end (midway between split ends).

Static deflection and dynamic test data from Blade S/N 001 tests, conducted immediately after the failure and before repair, was noticeably different when compared to the data accumulated before the damage. Deflections and the displacements were considerably larger and the natural frequencies were lower. The same tests conducted after the repairs were made yielded data very similar to the test data before the damage occurred, indicating the blade had been restored to its original condition. See Tables 5, 6, 8 and 9. Static test sequence number 4

and dynamic test sequence 5 were conducted immediately after damage. Static test sequence number 7 and dynamic test sequence 8 were conducted after repairs.

The blade was very simply repaired by pouring a mixture of resin into the separation area and then clamping the area closed using a vacuum bag around the blade. Resin was also injected into the fringes of the damaged area where the poured resin could not reach.

Figure 27 is a photograph of the damage as seen during post failure flapwise static deflection tests.

Table 10 summarizes the blade tip deflections at proof loads.

TABLE 4 - STATIC DEFLECTION AND CREEP TEST RESULTS - FLAPWISE

Blade	Test Sequence Number	Sta. No...	Leading-Edge Deflection (in.) 88	138	188	238	284	Trailing-Edge Deflection (in.) 88	138	188	238	284
001	1		.33	1.95	4.75	8.83	11.83	.29	1.89	4.69	8.33	11.78
001	4		.40	2.03	4.99	8.80	12.53	-	1.87	4.94	8.75	11.81
001	7		.29	1.77	4.39	8.12	11.01	.27	1.90	4.39	7.72	11.01
001	10		.44	2.04	4.84	8.39	11.98	.36	2.00	4.88	8.44	12.04
002	1		.35	1.88	4.49	7.85	11.27	.033	1.82	4.52	7.90	11.27
002	4		.29	1.66	4.01	7.01	10.06	.27	.64	3.99	7.04	11.11
002	7		.34	1.98	4.77	8.15	11.97	.35	2.02	4.80	7.97	12.08
002	10		.34	1.86	4.50	7.93	11.32	.30	1.86	4.52	7.93	11.43
002	13		.36	2.12	5.14	9.03	12.95	.35	2.15	5.17	9.07	12.98
002	16		.33	1.85	4.47	7.83	11.21	.30	1.77	4.49	7.88	11.25
002	20		.67	2.51	5.49	9.27	12.80	.62	2.50	5.49	9.30	12.90
003	1		.36	1.50	3.41	5.87	8.36	.35	1.48	3.42	5.83	8.33
003	4		.26	1.39	3.31	5.35	8.25	.23	1.38	3.31	5.76	8.25
003	7		.30	2.06	3.57	6.18	8.84	.27	1.51	3.76	6.20	8.88

TABLE 5 - STATIC DEFLECTION AND CREEP TEST RESULTS - CHORDWISE

Blade	Sequence Number	Station No.	Chordwise Deflection (in.) 38	138	188	238	284
001	1		.09	.30	.70	1.12	1.65
001	4		.45	1.16	2.22	3.54	5.03*
001	7		.08	.32	.70	1.14	1.63
001	10		.07	.29	.65	1.09	1.52
002	1		.07	.24	.62	1.21	1.65
002	4		.10	.32	.71	1.29	1.84
002	7		.10	.38	.85	1.46	2.07
002	10		.08	.28	.63	1.07	1.51
002	13		.08	.31	.63	1.09	1.54
002	16		.07	.31	.71	1.22	1.70
002	20		.10	.34	.73	1.20	1.67
003	1		.13	.36	.67	1.04	1.45
003	4		.04	.01	.46	.67	1.12
003	7		.08	.25	.54	.88	1.28

* Measured after chordwise damage.

TABLE 6 - STATIC DEFLECTION AND CREEP TEST RESULTS - TORSIONAL

Blade	Sequence Number	Station No.	Rotation (degrees) 88	138	188	238	284
001	1		.87	2.40	3.60	4.91	6.22
001	4		1.44	2.64	4.01	4.94	6.46
001	7		.82	2.70	3.84	4.66	6.38
001	10		.90	2.13	3.57	4.72	6.55
002	1		.41	1.38	3.76	5.84	7.32
002	4		1.09	2.67	4.09	5.56	7.01
002	7		.87	2.56	3.98	4.39	6.57
002	10		.95	1.99	4.20	5.62	6.90
002	13		1.09	2.67	3.93	5.64	7.25
002	16		1.01	2.56	4.04	5.70	6.80
002	20		1.44	2.91	4.41	6.22	7.61
003	1		.98	2.20	3.62	5.10	6.24
003	4		.68	2.18	3.62	5.15	6.24
003	7		.98	2.67	3.46	4.88	6.22

TABLE 7 - DYNAMIC TEST RESULTS - FLAPWISE

Blade	Test Sequence Number	Mode	Frequency (Hz)	Tip Disp.	1st Node Loc.	2nd Node Loc.	1st Antinode Loc.	1st Antinode Disp.	2nd Antinode Loc.	2nd Antinode Disp.
001	2	1	1.06	12.8						
001	5	1	1.06	12.0						
001	8	1	1.06	13.0						
001	11	1	1.06	9.0						
002	2	1	1.06	11.1						
002	5	1	1.06	11.0						
002	8	1	1.10	10.0						
002	11	1	1.06	10.0						
002	14	1	1.06	11.0						
002	17	1	0.76	11.5						
002	19	1	1.06	11.0						
003	2	1	1.20	1.68						
003	5	1	1.20	1.60						
003	8	1	1.20	2.10						
001	2	2	6.0	2.80	214		140	1.6		
001	5	2	6.0	1.70	214		150	1.6		
001	8	2	6.0	5.00	214		140	4.2		
001	11	2	6.0	1.80	214		146	1.1		
002	2	2	6.5	0.45	196		98	0.32		
002	5	2	6.5	0.50	217		165	0.52		
002	8	2	6.5	1.30	215		135	0.85		
002	11	2	6.5	0.80	216		134	0.70		
002	14	2	6.5	1.00	216		132	1.10		
002	17	2	6.5	1.20	216		132	1.10		
002	19	2	-	-	-		-	-		
003	2	2	7.0	1.00	214		127	0.75		
003	5	2	7.0	4.00	210		127	2.60		
003	8	2	7.0	5.20	214		126	3.00		
001	2	3	17.0	4.50	150	231	89	3.8	190	1.8
001	5	3	17.0	2.50	156	225	96	3.0	196	0.7
001	8	3	17.0	3.80	150	230	96	3.5	190	2.0
001	11	3	16.1	2.70	147	232	88	1.8	190	1.0
002	2	3	16.0	5.25	151	231	85	3.8	191	2.3
002	5	3	17.0	1.8	152	230	88	1.7	184	1.1
002	8	3	17.0	2.0	152	229	98	1.6	186	1.1
002	11	3	17.0	3.4	152	228	98	3.4	188	2.0
002	14	3	17.0	2.0	152	230	86	2.0	184	1.1
002	17	3	17.0	1.9	152	230	86	1.4	184	1.8
002	19	3	-	-	-	-	-	-	-	-
003	2	3	19.0	4.0	145	232	89	3.5	188	2.30
003	5	3	19.0	3.0	146	232	93	3.2	191	1.32
003	8	3	19.0	4.0	146	231	93	3.0	189	2.20

Note: The large differences in tip deflection and 1st Antinode displacements are due to variation in input displacement, not changes in the blades.

TABLE 8 - DYNAMIC TEST RESULTS - CHORDWISE

Blade	Test Sequence Number	Frequency (Hz)	Tip Displacement (in.)
001	2	5.5	0.65
001	5	4.0	1.20
001	8	7.0	0.45
001	11	6.0	0.50
002	2	5.0	0.52
002	5	6.0	0.42
002	8	5.0	0.50
002	11	5.0	0.60
002	14	6.0	0.80
002	17	6.0	0.80
002	19	-	-
003	2	6.0	0.50
003	5	6.0	0.45
003	8	6.0	0.30

TABLE 9 - DYNAMIC TEST RESULTS - TORSIONAL

Blade	Test Sequence Number	Mode	Frequency (Hz)	Tip Displacement (in) D. A.	Node Loc.	Antinode Location	Antinode Displacement
001	2	1	21	1.20			
001	5	1	18	1.50			
001	8	1	19	1.10			
001	11	1	19	1.00			
002	2	1	16	0.63			
002	5	1	17	1.30			
002	8	1	20	3.20			
002	11	1	20	3.00			
002	14	1	19	3.80			
002	17	1	19	3.0			
002	19	1	20	3.5			
003	2	1	21	1.88			
003	5	1	21	1.66			
003	8	1	21	2.10			
001	2	2	59	1.00	180		
001	5	2	63	0.60	184	120	
001	8	2	62	0.80	191	123	
002	2	2	61	0.40	180	110	0.49
002	5	2	58	1.30	190	83	1.80
002	8	2	60	1.50	190	90	1.60
002	11	2	59.5	1.00	190	100	1.20
002	14	2	60	0.80	191	86	1.00
002	17	2	60	0.80	191	86	1.00
002	19	2	57	1.00	188	86	1.00
003	2	2	66	2.00	190	90	1.50
003	5	2	66	0.50	175	94	0.80
003	8	2	68	0.80	204	102	0.70

TABLE 10 - BLADE TIP DEFLECTION - PROOF LOAD

Condition	S/N 001	S/N 002	S/N 003
Flapwise L. E., in.	70.41	69.19	58.21
Flapwise T. E., in.	70.81	69.72	59.47
Chordwise, in.	*	7.17	5.15
Torsion, deg	14.27	15.82	12.98

* Blade failed at 1650 pounds tip load (2.16 times limit), and no measurement was taken.

FATIGUE TESTS

The fatigue test data is summarized in Table 11 and Figures 28, 29 and 30.

TABLE 11 - FATIGUE TEST DATA SUMMARY

Blade	Maximum Strain (in./in.)	Number of Cycles	Frequency (Hz)
S/N 001	±.003472	217,958	16
	±.001650	1,009,661	16
S/N 002	±.000920	450,000	17
	±.001100	167.076	17
	±.001670	350,676	17
	±.002360	39,326	17
	±.002360	116,000	13
S/N 003	±.000680	450,000	19
	±.001240	350,000	19
	±.001750	200,000	19

After 217,958 cycles at a maximum skin strain of ±.003472 in./in. the skin in the root end failed. The failure was noticed by a change in sound, and the natural frequency abruptly dropped from 17.1 to 16.0 Hz. The failure began at the center of the 2.5-inch pin hole and progressed toward the leading and trailing edges on both sides of the blade. The damaged area appeared as a discolored, bulging line resulting from the delamination of the composite and fatigue failure of the stainless steel laminate. The general area of the failure was hot (approximately 260°F). The test strain level was reduced to ±.001650 in./in., and the test continued at this level for 10^6 more cycles without further failure. A fan was placed to blow air across one side of the root end during the last portion of the test to dissipate the heat. The temperature stabilized at 110°F

Blade S/N 002 withstood 450,000 cycles at a strain of ±.00920 in./in., 167,076 cycles at a strain of ±.001200 in./in., 350,000 cycles at a strain of ±.001670 in./in., and 29,376 cycles at a strain of ±.002360 in./in. The ±.001200 level was performed in error. At 29,376 cycles of the high level (±.002360 in./in. strain) test, a fatigue falure appeared in the root end 5 inches from the center of the 2.5-inch pin hole toward the blade tip (see Figure 31). Testing was continued for an additional 116,000 cycles until failure progressed to the point where vibration could no longer be effectively induced. A total of 1.112×10^6 cycles was accumulated on the blade. The blade natural frequency in this mode was 17 Hz before the failure. After the failure, it was 15 Hz and gradually reduced to 13 Hz when the test terminated.

The fatigue line when first seen was 6 inches long. As the test continued the line gradually extended toward the trailing edge and was approximately 16 inches long when the test was terminated.

It was noted during the testing of S/N 002 that the laminated area around the large pin moved in a breathing motion relative to the pin. Displacement was approximately 0.25 inch. This motion probably occurred on all blades, at least to some extent. Reasons for this include the method of mounting the blade and also the fit of the large pin. A bolt instead of the pin allowing a clamping attachment would probably not have allowed damage to occur. The pin in Blade S/N 003 (blade not damaged) fitted tighter than the pins in the other two blades. The damage to the two blades is attributed to these two factors and the high strain test levels.

ULTIMATE TESTS

The blade tip deflection (average of leading and trailing edges) versus load is shown in Figure 32.

S/N 001

S/N 001 failed at a tip height (leading edge) of 10 feet above the zero position with a loading of 750 pounds. Failure occurred in the root end beginning at the damaged area incurred during fatigue testing. The failure line began at the center of the 2-1/2-inch-diameter hole, progressed straight to the leading edge, made an abrupt right angle turn at the seam in the leading edge, and progressed toward the tip for about 2-1/2 feet. The load after breakage dropped to 600 pounds (see Figures 33 and 36).

S/N 002

S/N 002 ultimate testing was terminated at a tip leading edge height of 144 inches above zero and a loading of 915 pounds. The test was terminated at this point because the blade was hinging at the damaged section of the root end sustained during fatigue testing (see Figures 35 and 37).

S/N 003

S/N 003's first major break occurred at a tip height of 120 inches and a loading of 975 pounds. The break consisted of skin compression failure at Station 84 and leading edge split from Station 35 to Station 76. When the break occurred, the load dropped immediately back to 850 pounds. Testing was continued to a height of 132 inches and 1100 pounds. At this time, the trailing edge split open from Station 48 to 96 and the load dropped to 950 pounds (see Figures 34 and 38).

BALLISTIC (BULLET IMPACT) TESTS

Results of the bullet impacts on Blade S/N 002 are described in detail in the appendix. Also see Figures 39 and 40.

Two bullets were fired into the leading edge of S/N 003. This first round, fired at a velocity of 1800 feet per second, caused less damage than expected (see Figure 39) so a round was fired at 2500 feet per second. In both cases the bullets cut the skin and glanced off the longo material, leaving a shallow groove. The higher velocity round resulted in noticeably more damage to the surrounding skin (see Figures 41 and 42).

The bullet fired into the trailing edge on Blade S/N 003 penetrated through the blade and lodged, partially exposed, on the back side. The bullet hole was 3.3 inches long on the entrance side and 4.9 inches long on the exit side. The damage extended to a width of approximately 1.5 inches on each side of the hole.

Bullet impact damage (.30 caliber) was very slight, causing almost no change in blade response.

SIMULATED TREE STRIKE TESTS

No damage was sustained by either of the two blades tested as a result of the tree strike tests (see Figure 43). The blades have excellent resistance to damage from simulated tree strikes.

BALL DROP TESTS

The fiberglass blade (S/N 002) withstood the impact of the steel ball with noticeably less effect than the PRD-49 (S/N003) blade. No damage was visible on the fiberglass blade after drops of up to 17 feet except for small dents resulting from the highest drops. These dents reached a maximum depth of .012 inch in the fiberglass blade and .025 inch in the PRD-49 blade. The largest dents resulted from drops close to the trailing edge. Drops on the PRD-49 blade resulted in minor fracturing of the skin at drop heights of 8 and 9 feet. In no case did the ball penetrate the skin. All damage was confined to the dented area where the ball hit. Figure 44 shows Blade S/N003 after the ball drop tests. The blades were found to have excellent resistance to ball drop impact damage.

CONCLUSIONS

1. The damage repair procedures were found to be 100% effective, inexpensive, and easily accomplished using hand tools only. The weakest portion of the blade was the metal shim area at the root end. The loose fit of the large attaching pin and the lack of clamping action were felt to contribute greatly to the root end damage experienced on S/N 001 and S/N 002.

2. There were no indications of changes in the blades other than at the root end as a result of testing.

3. The blades are capable of withstanding extremely large flapwise tip deflections (up to 10 feet) without damage. The blades withstood from 300 to 500% of the design flapwise bending load.

4. The blades do not fail catastrophically. Even in the damaged condition after the ultimate loading test the blades are felt to be capable of sustaining flight loads as evidenced by only nominal changes in frequency and the remaining structural integrity.

RECOMMENDATION

Additional development of root end attachment techniques eliminating the interleaved metal shims is needed.

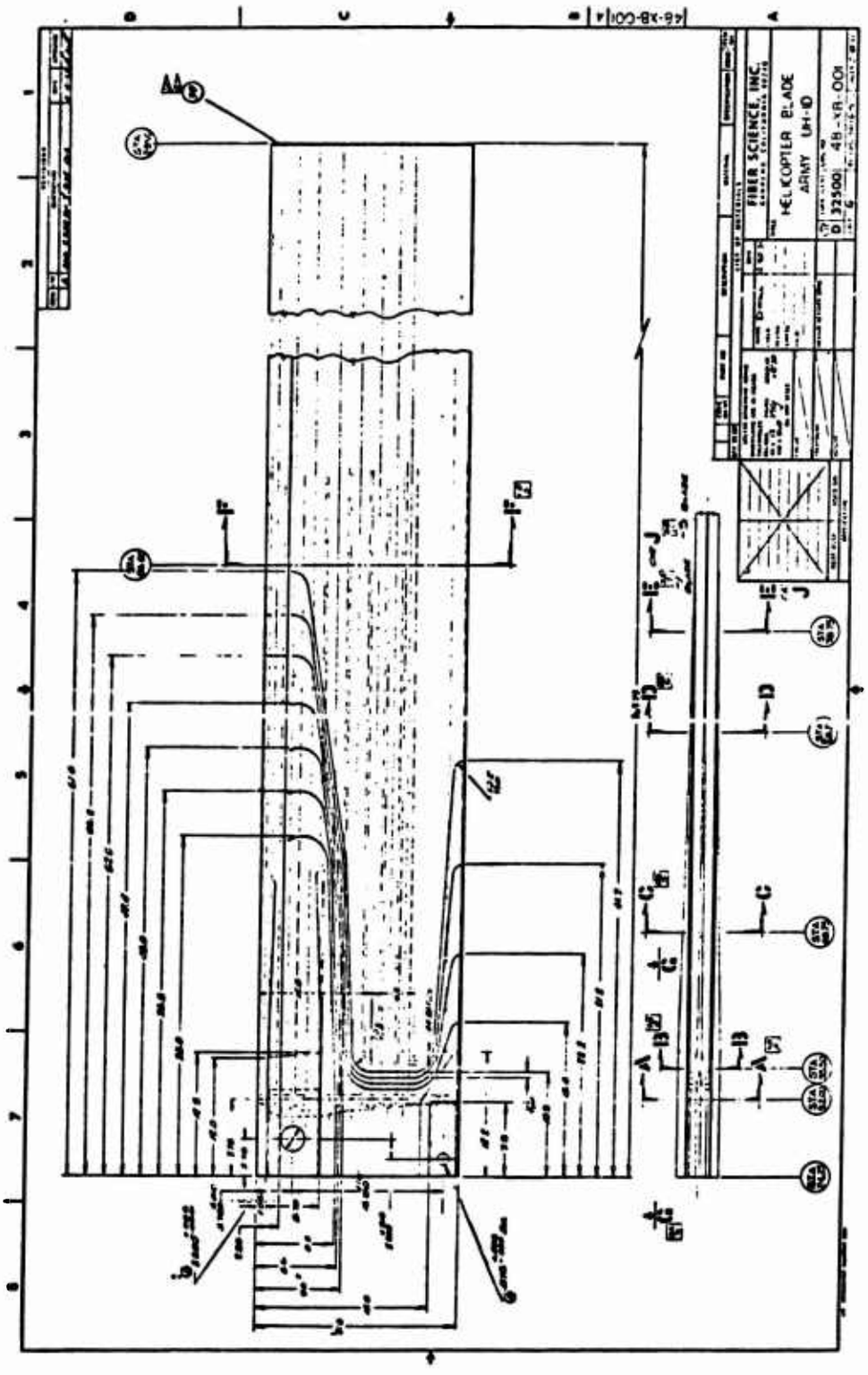

Figure 1. Army UH-1D Helicopter Blade.

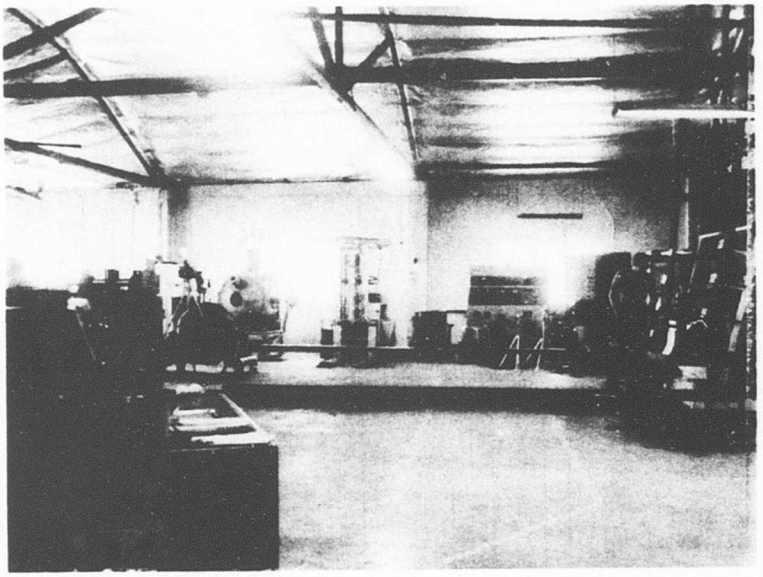

Figure 2. Flapwise Static Deflection and Creep - No-Load Condition.

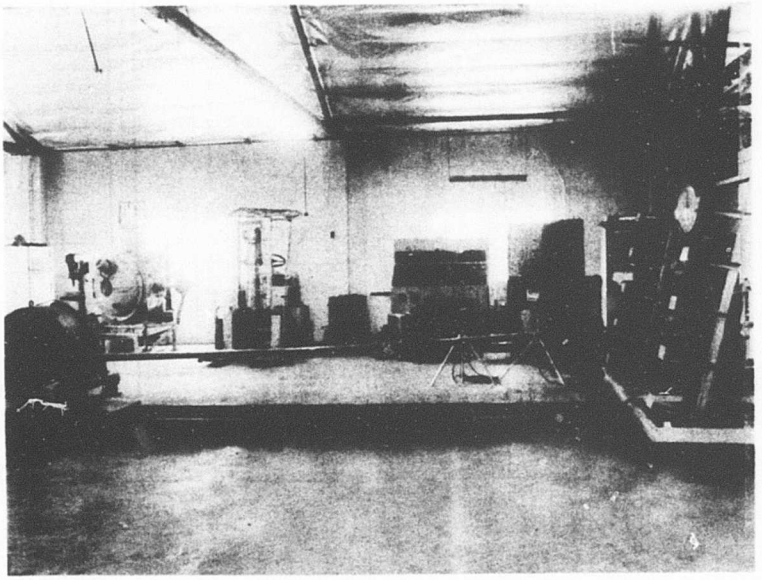

Figure 3. Flapwise Static Deflection and Creep - 50-Pound Load.

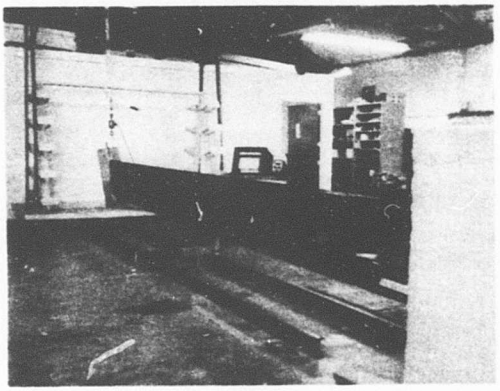

Figure 4. Chordwise Static Deflection and Creep - Loaded Condition.

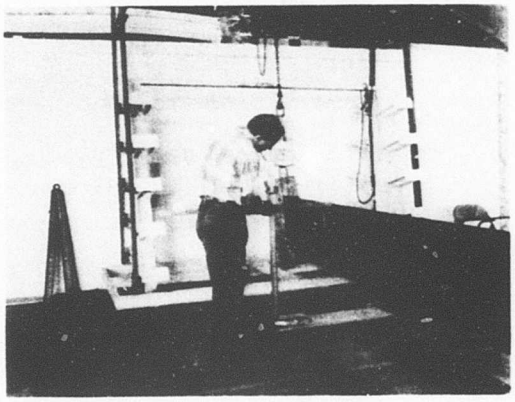

Figure 5. Chordwise Creep Measurement.

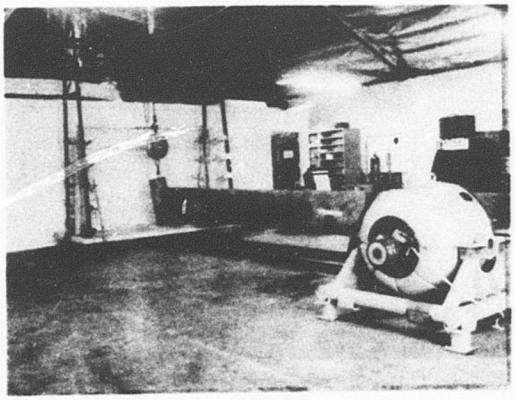

Figure 6. Chordwise Creep Loaded Condition - S/N 003.

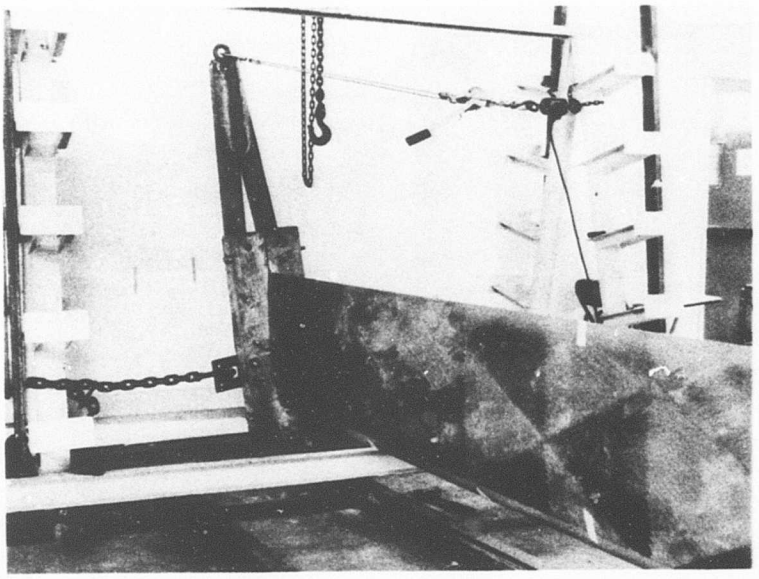

Figure 7. Torsional Static Deflection and Creep - No Load.

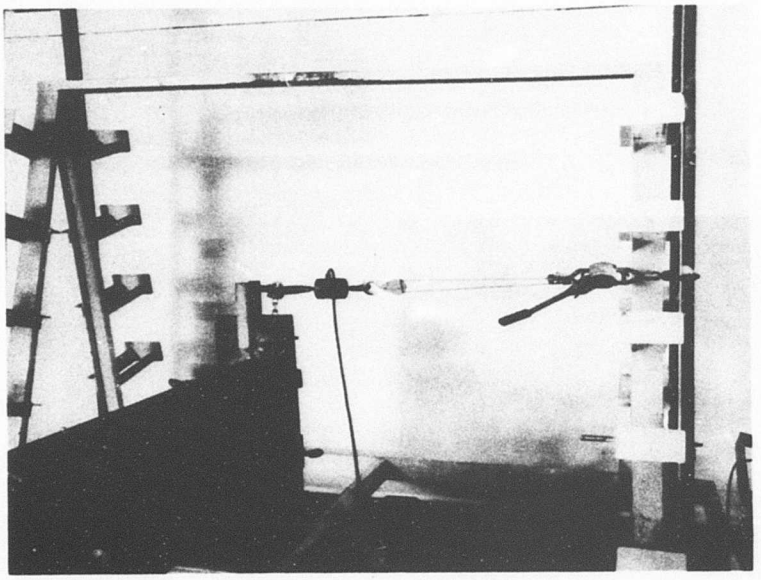

Figure 8. Torsional Static Deflection and Creep - Loaded Condition.

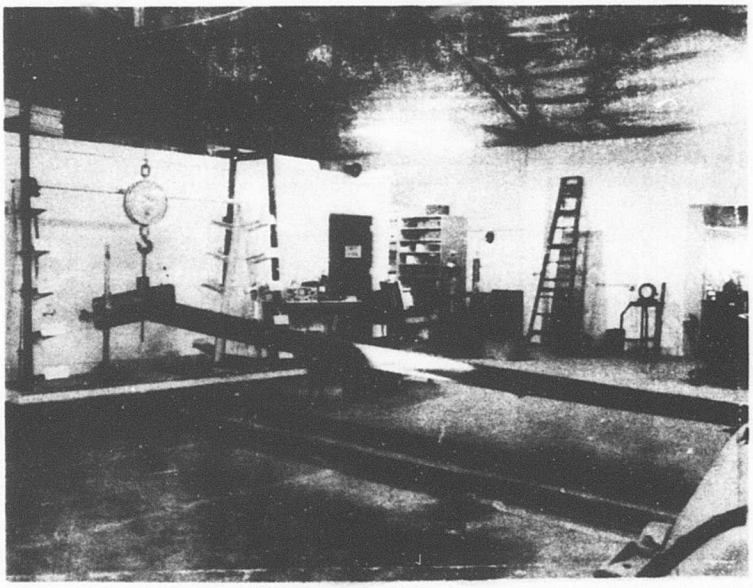

Figure 9. Deflection Measurement Technique.

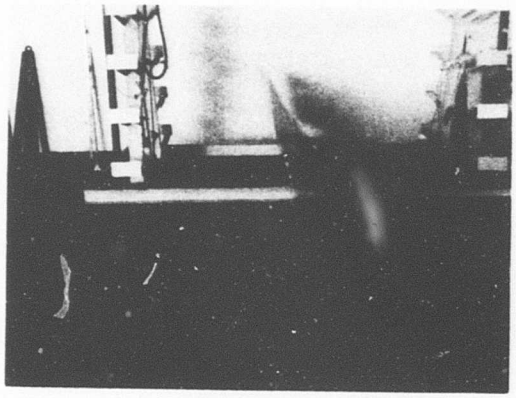

Figure 10. Flapwise Dynamic Test.

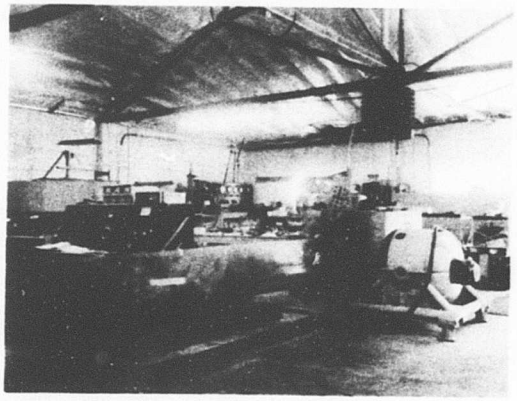

Figure 11. Chordwise Dynamic Test.

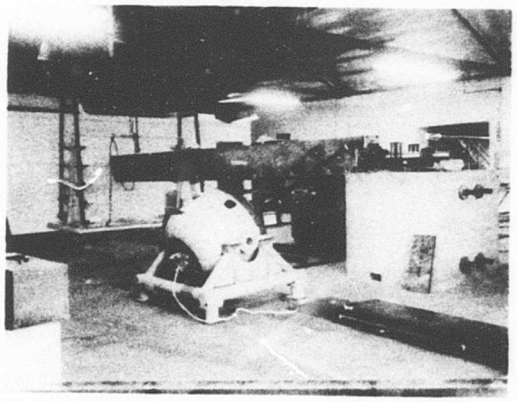

Figure 12. Torsional Dynamic Test.

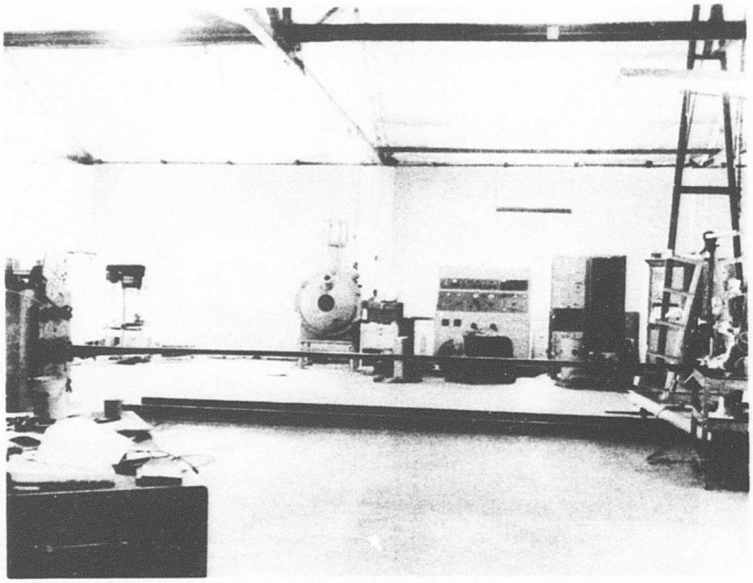

Figure 13. Flapwise Proof - Zero Position.

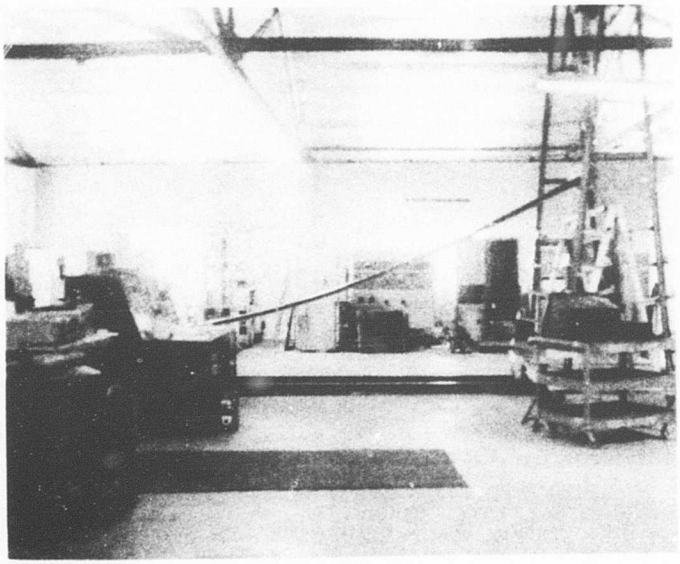

Figure 14. Flapwise Proof - Loaded Position.

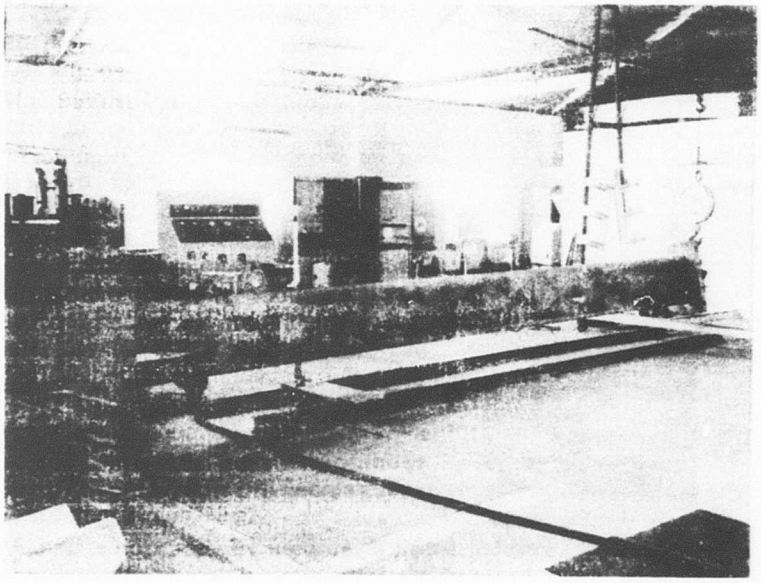

Figure 15. Proof Chordwise - Load Applied - S/N 003.

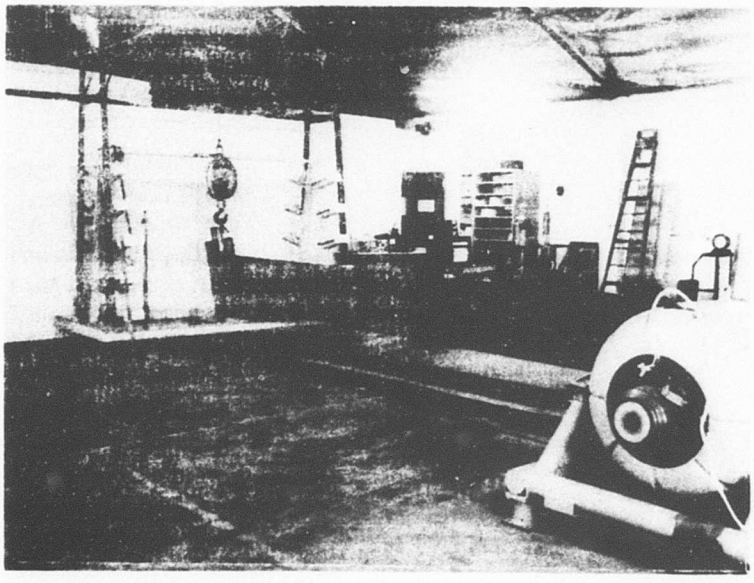

Figure 16. Proof Chordwise - No Load Applied - S/N 001.

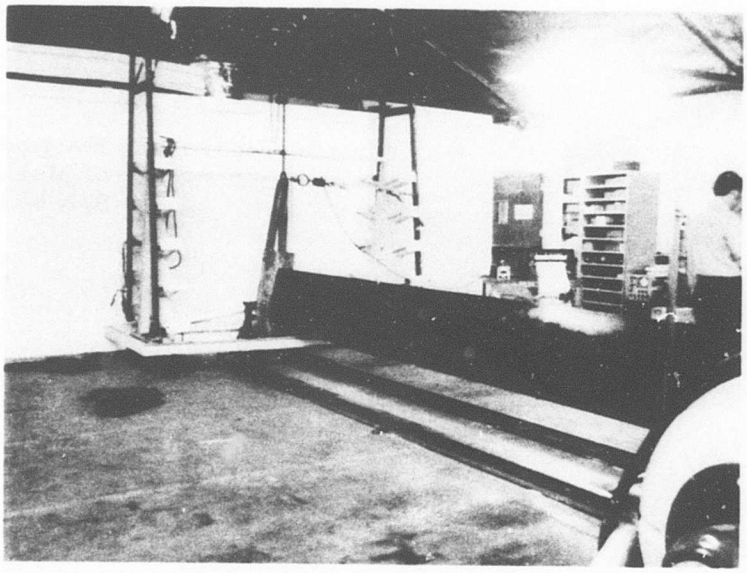

Figure 17. Proof Torsional - Load Applied - S/N 001.

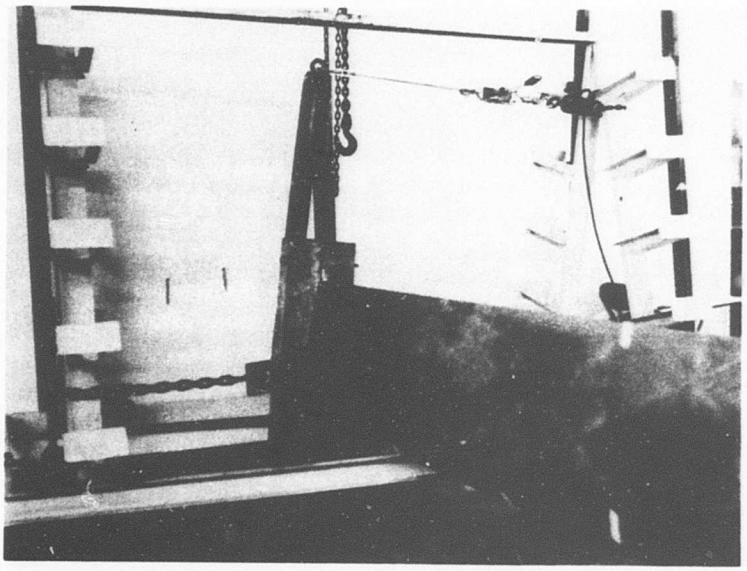

Figure 18. Proof Torsional - Load Applied - S/N 003.

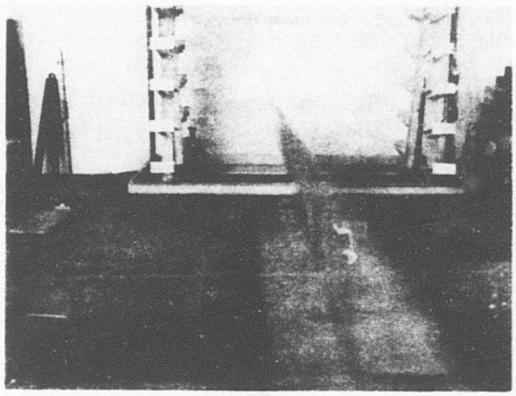

Figure 19. Fatigue Test - Area of Maximum Stress - S/N 003.

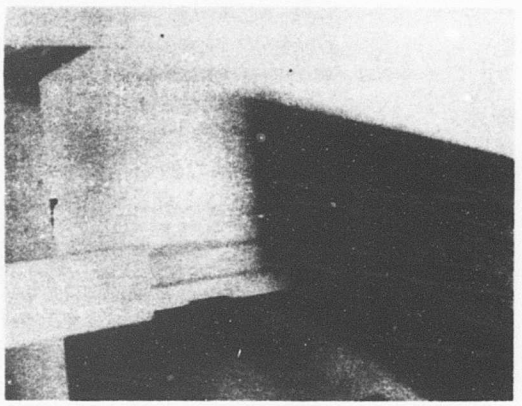

Figure 20. Fatigue Test - Tip Displacement.

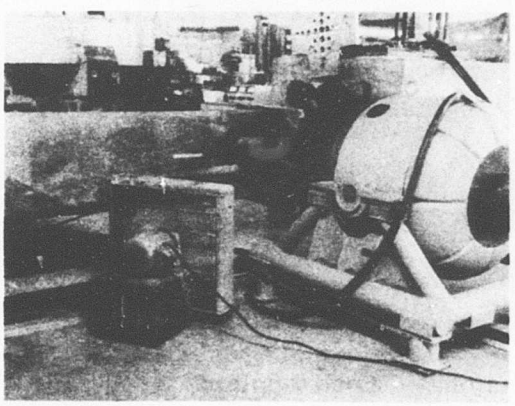

Figure 21. Fatigue Test - Root End Cooling - S/N 003.

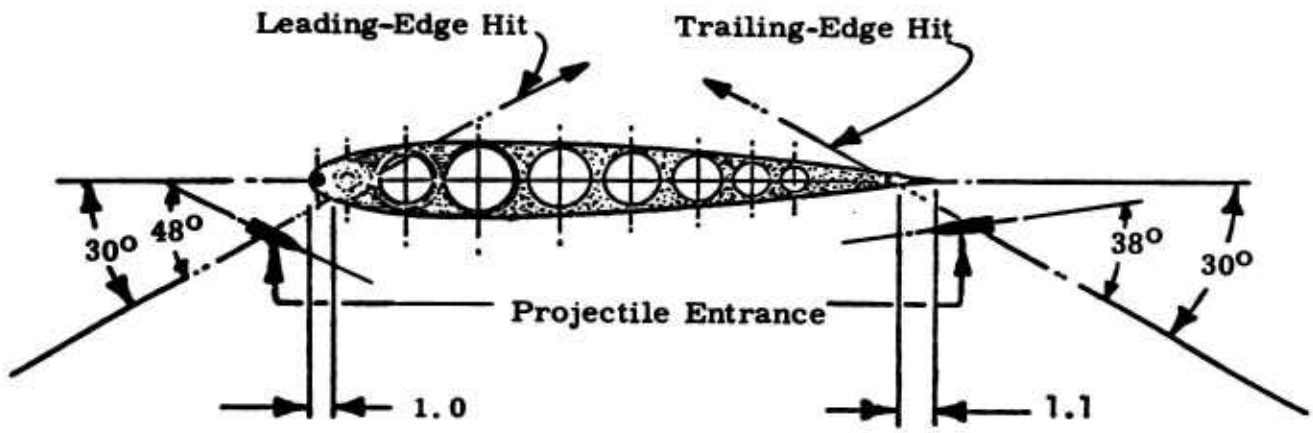

Figure 22. Ballistic Test - Bullet Projections.

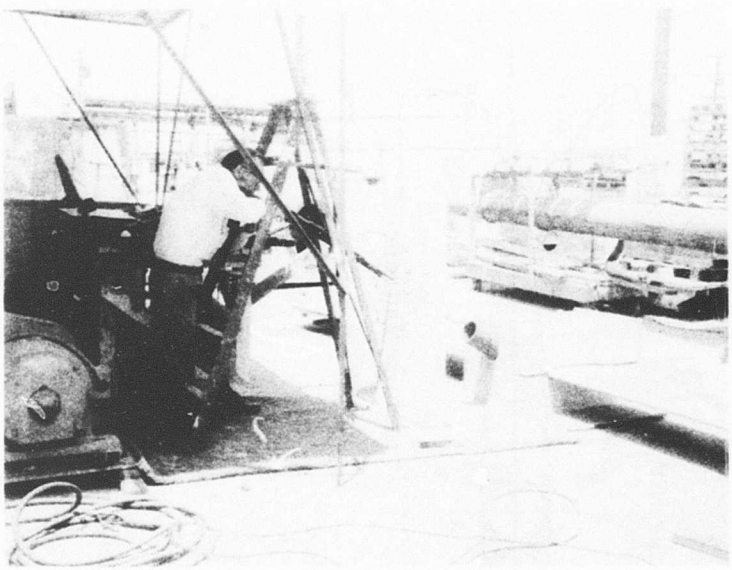

Figure 23. Bullet Impact Test Arrangement.

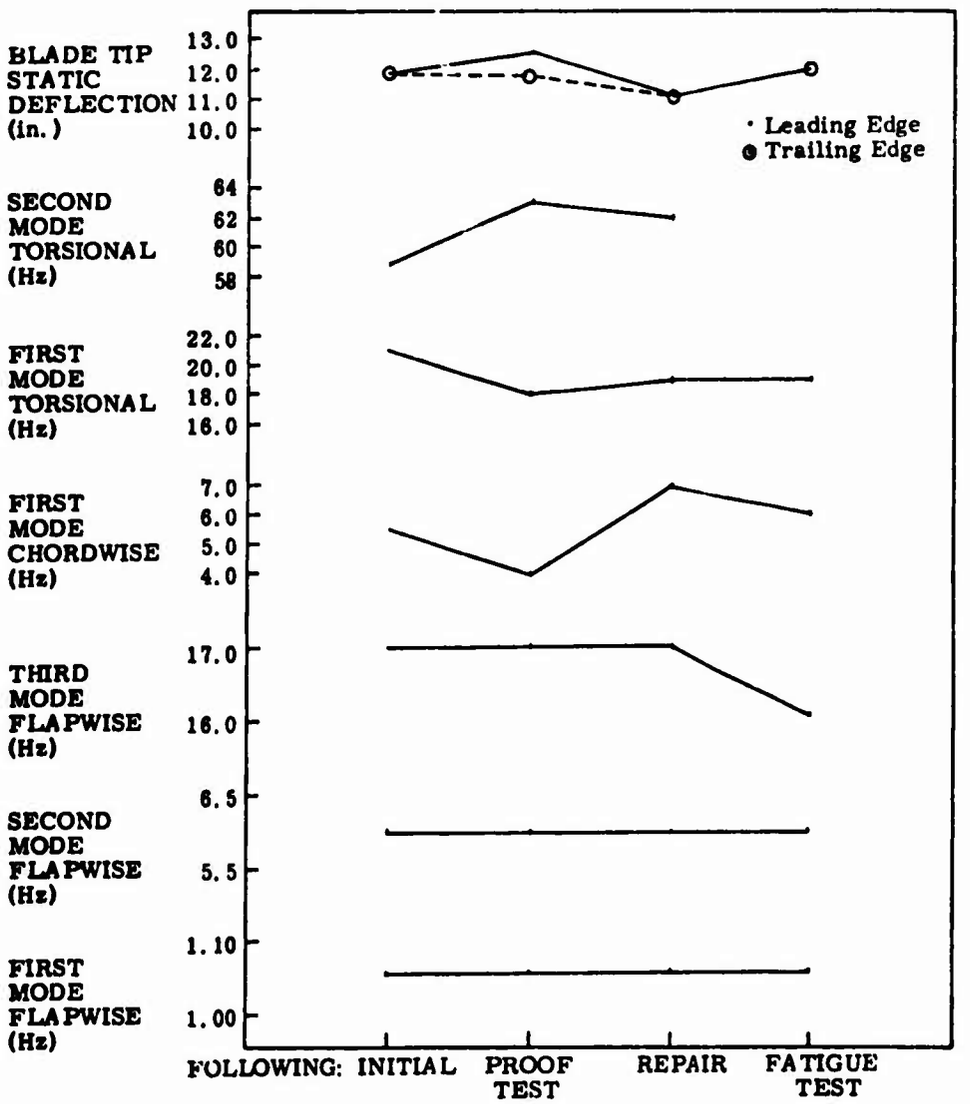

Figure 24. Static Deflection and Natural Frequencies Versus Test Sequence - S/N 001.

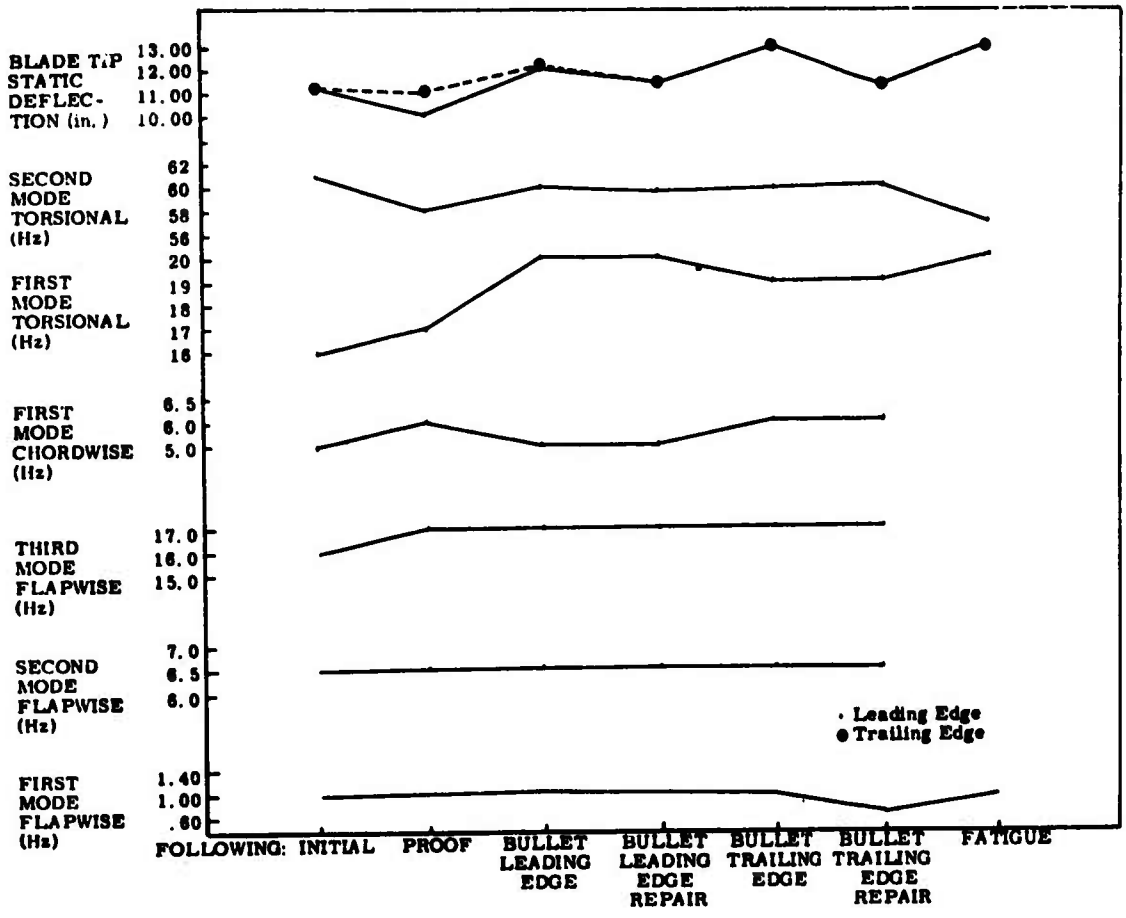

Figure 25. Static Deflection and Natural Frequencies Versus Test Sequence - S/N 002.

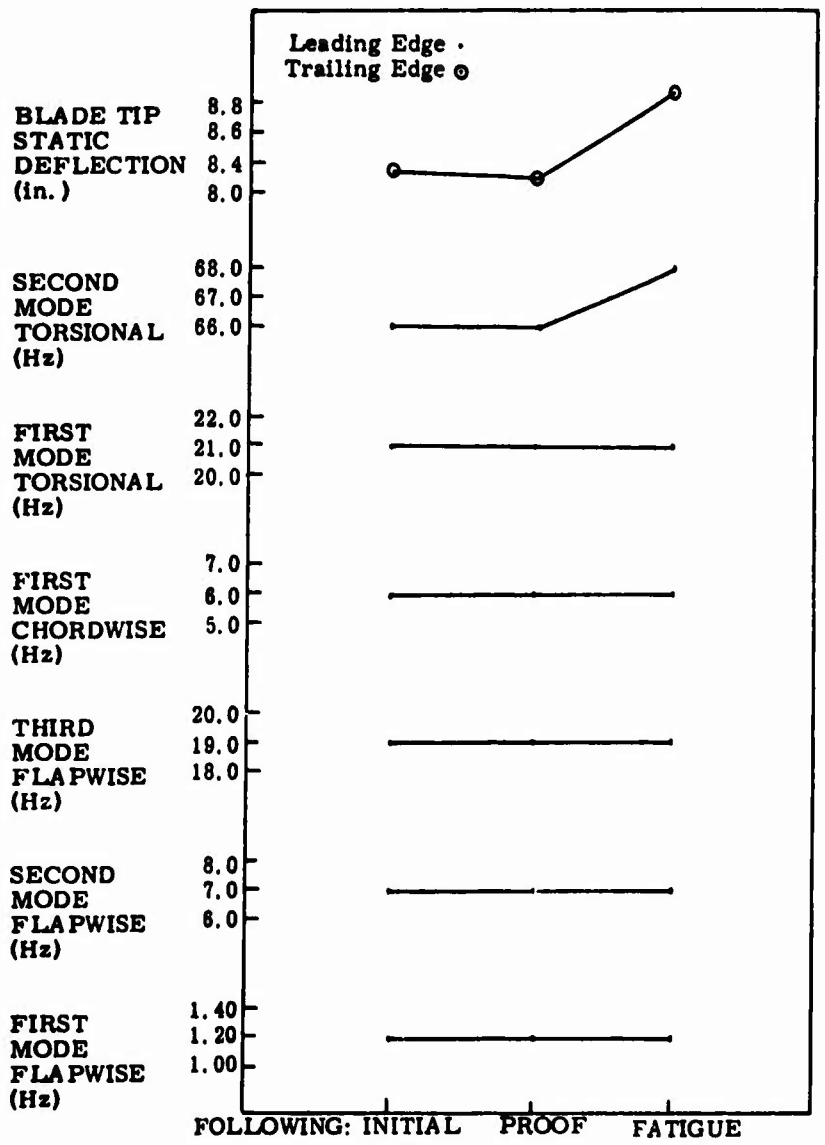

Figure 26. Static Deflection and Natural Frequencies Versus Test Sequence - S/N 003.

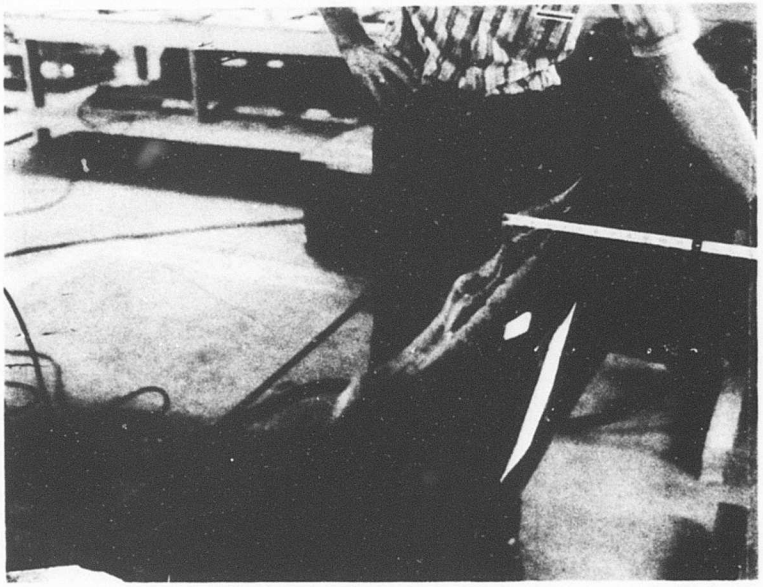

Figure 27. Chordwise Proof Test Failure - S/N 001.

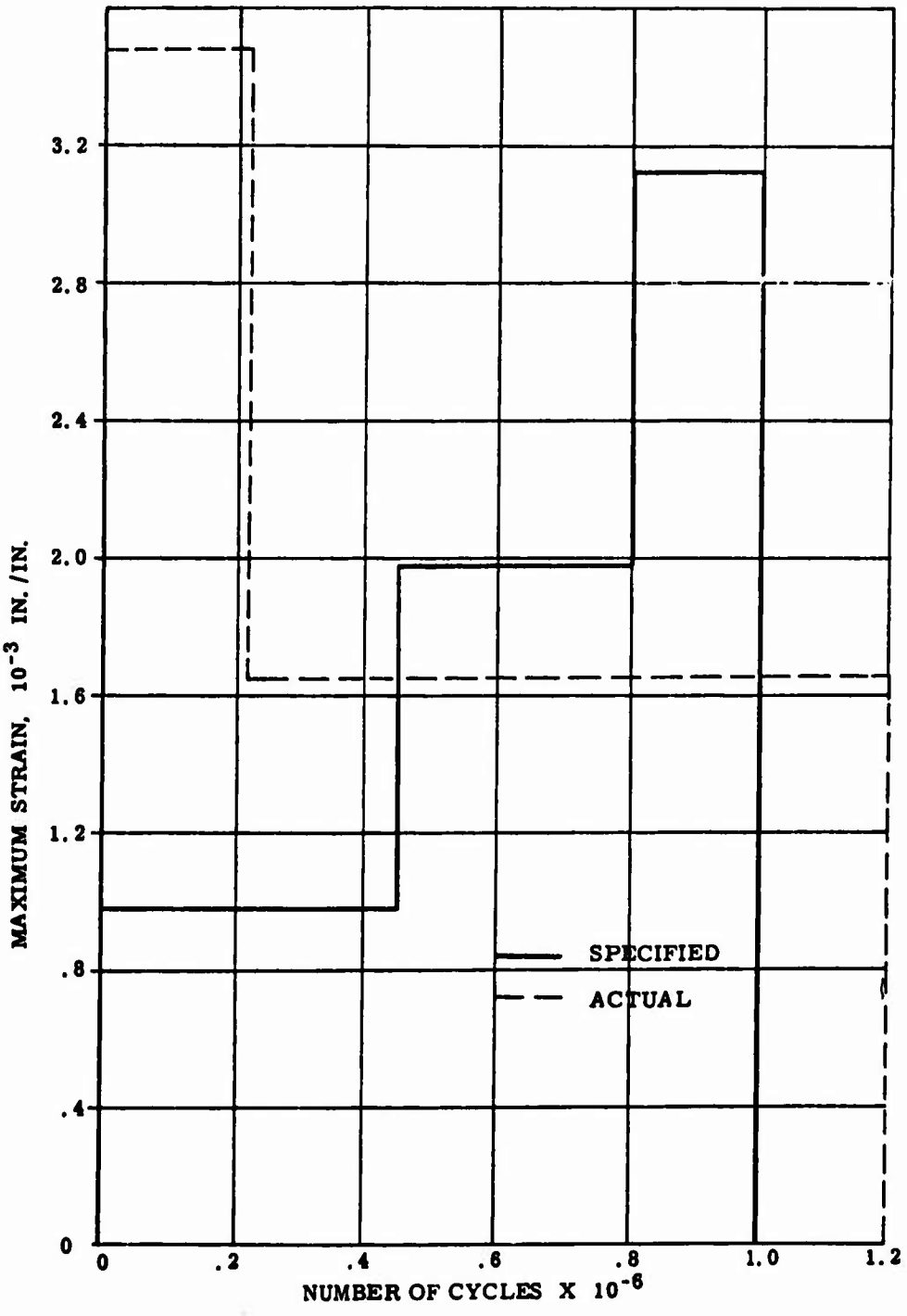

Figure 28. Fatigue Test Strain Levels Versus Number of Cycles - S/N 001.

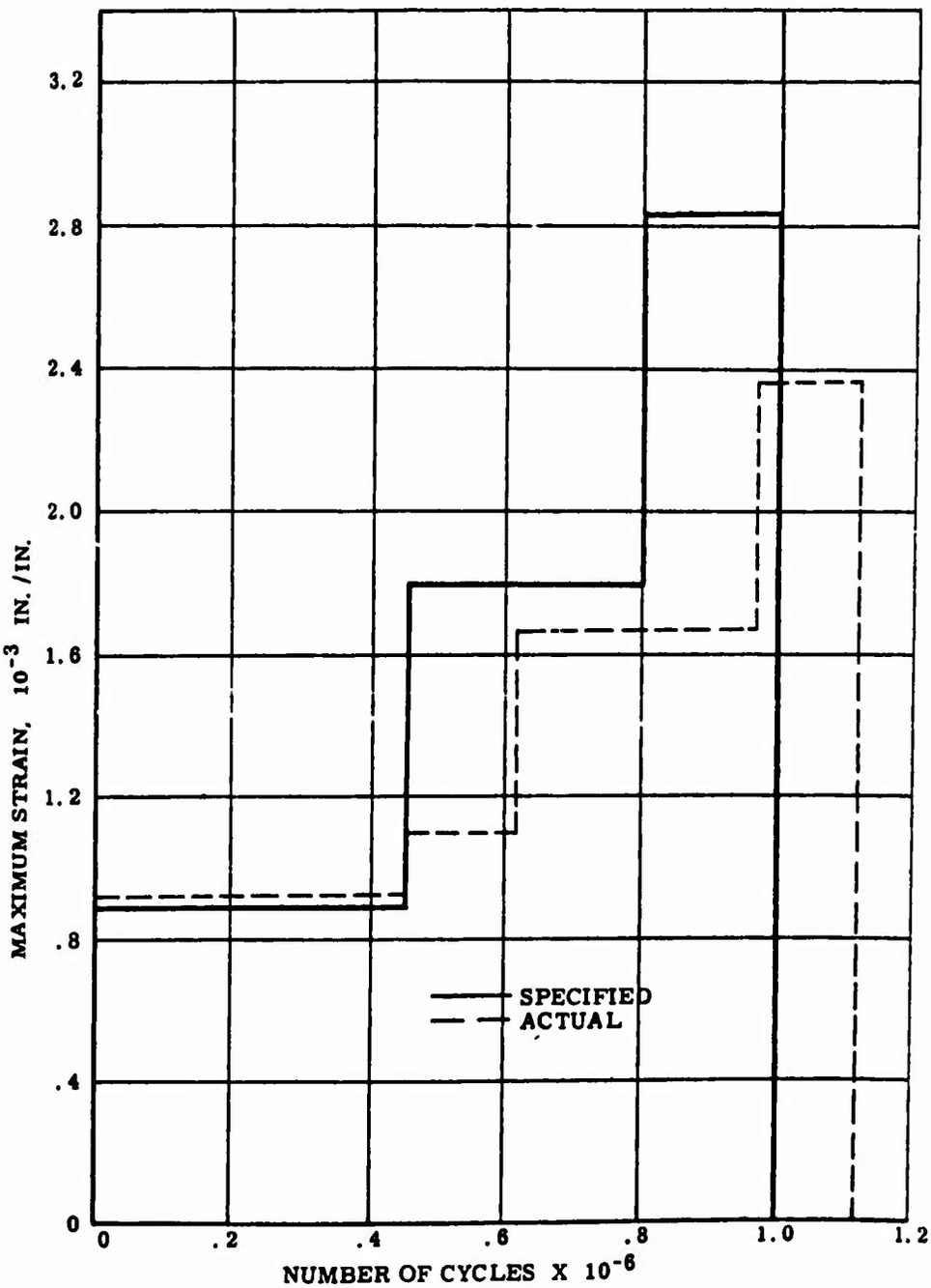

Figure 29. Fatigue Test Strain Levels Versus Number of Cycles - S/N 002.

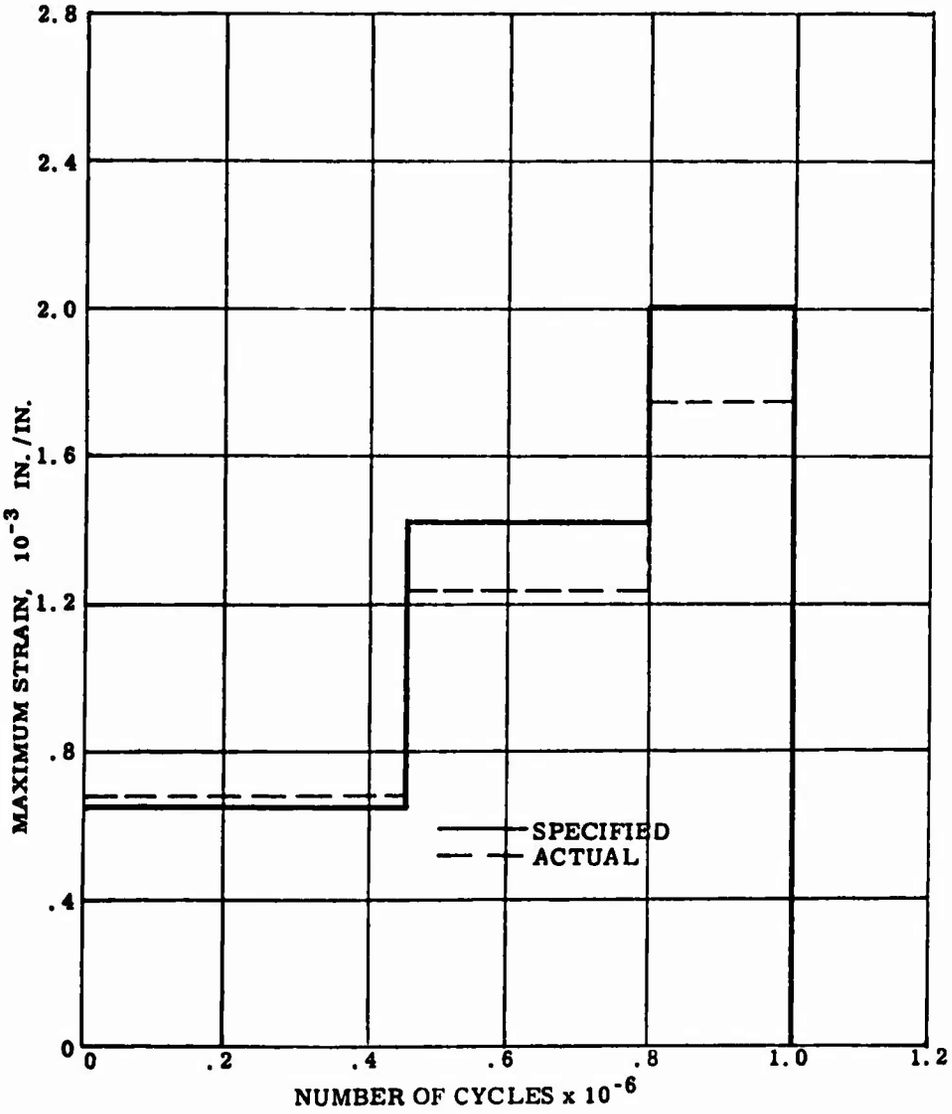

Figure 30. Fatigue Test Strain Levels Versus Number of Cycles - S/N 003.

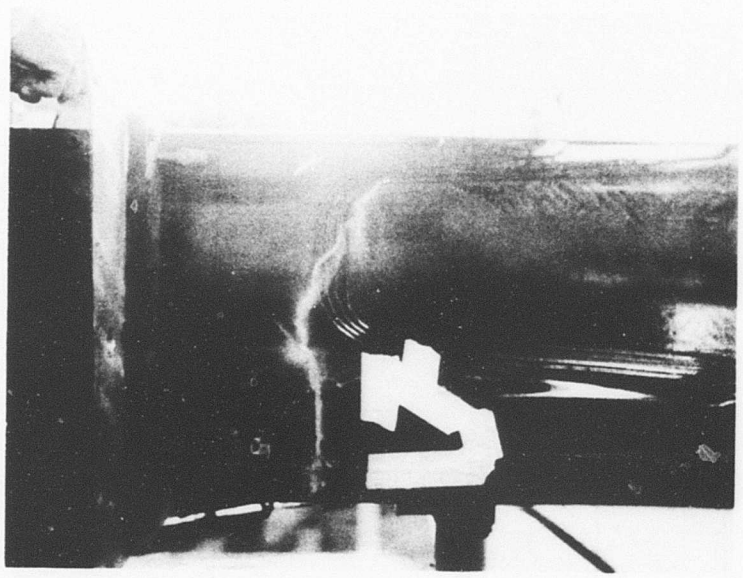

Figure 31. Fatigue Test Damage - S/N 002.

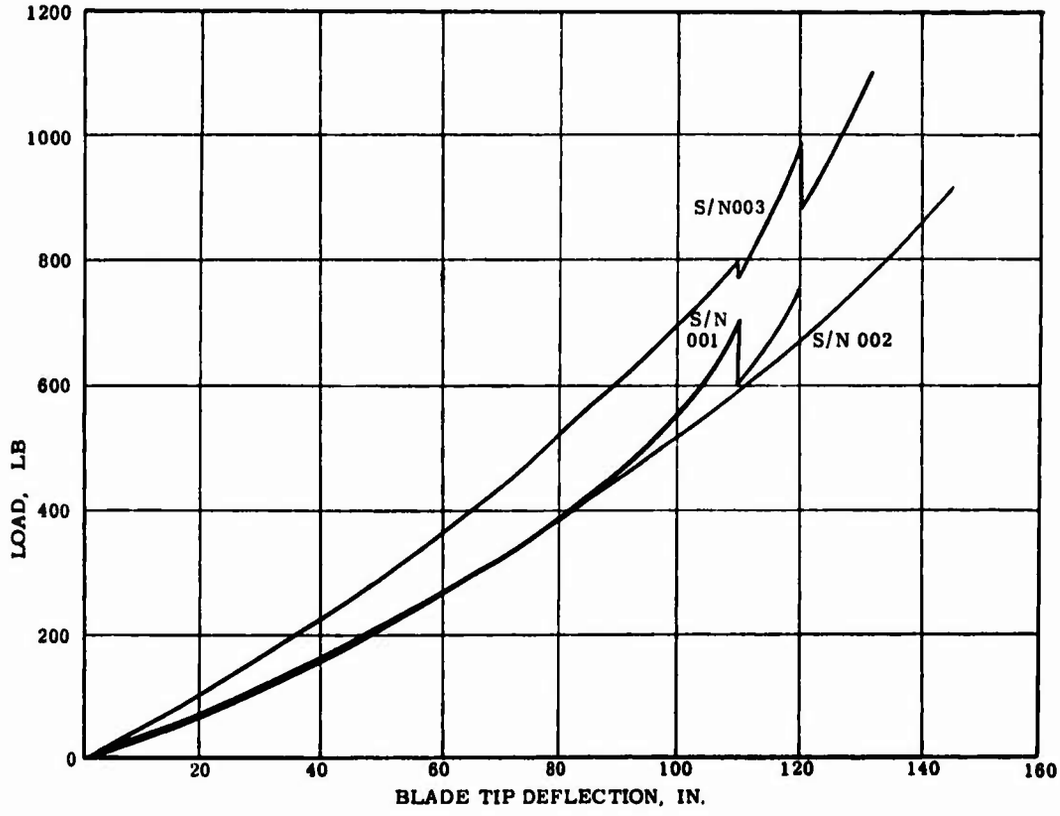

Figure 32. Load Versus Tip Deflection - Ultimate Beamwise Test.

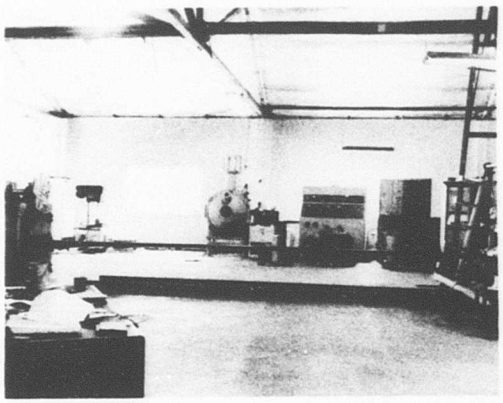

Figure 33. Ultimate Test - Typical Zero Position.

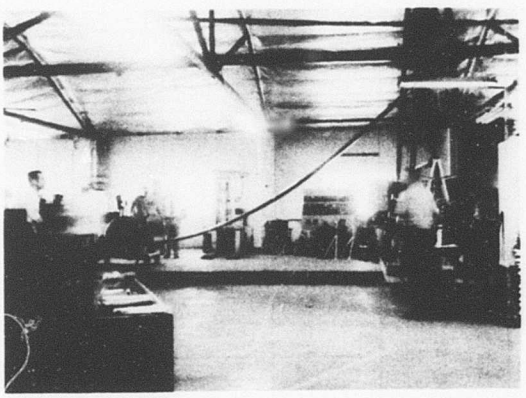

Figure 34. Ultimate Test - Maximum Loading at Break - S/N 003.

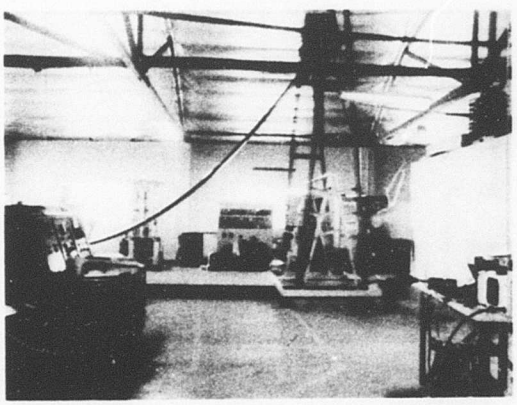

Figure 35. Ultimate Test - Maximum Loading at Break - S/N 002.

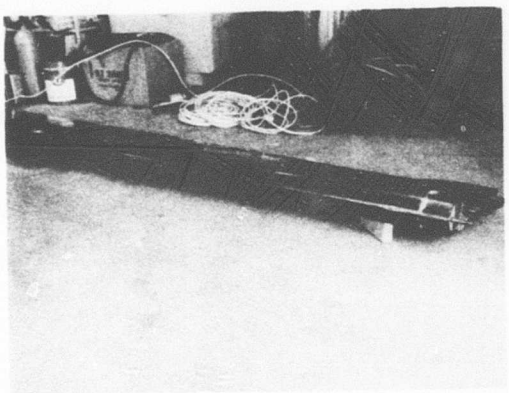

Figure 36. Ultimate Test Failure - S/N 001.

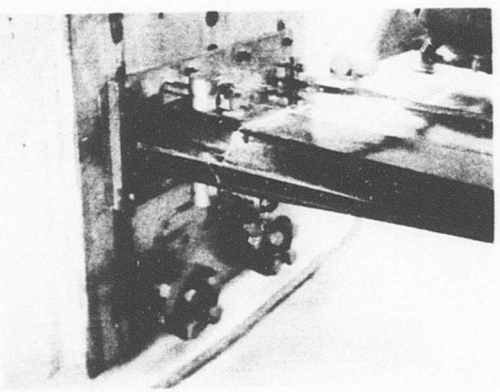

Figure 37. Ultimate Test Failure - S/N 002.

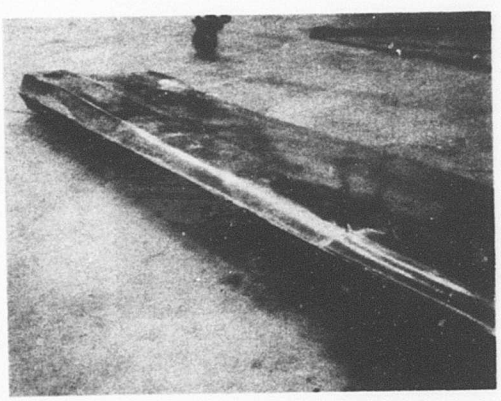

Figure 38. Ultimate Test Failure - S/N 003.

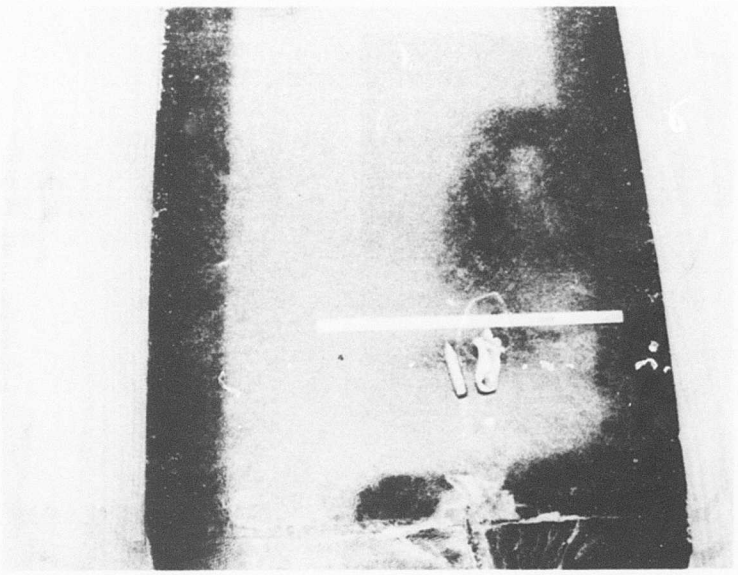

Figure 39. Bullet Impact, Leading Edge - S/N 002.

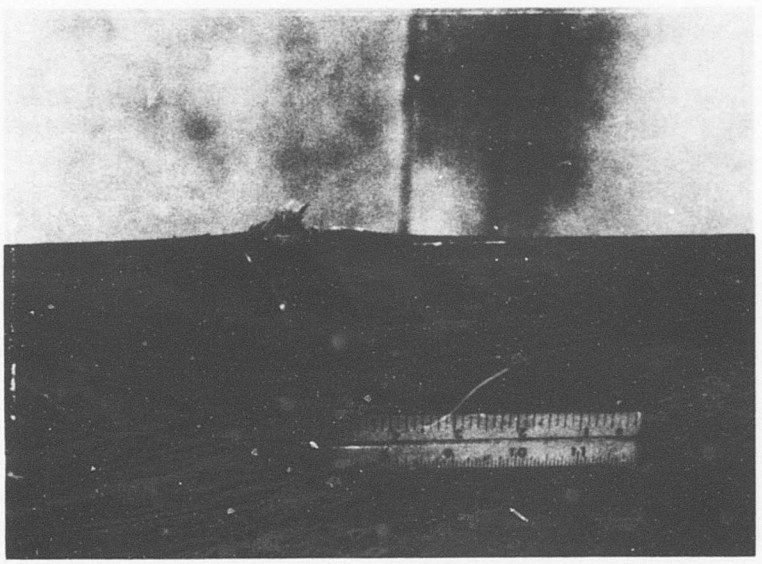

Figure 40. Bullet Impact, Trailing Edge - S/N 002.

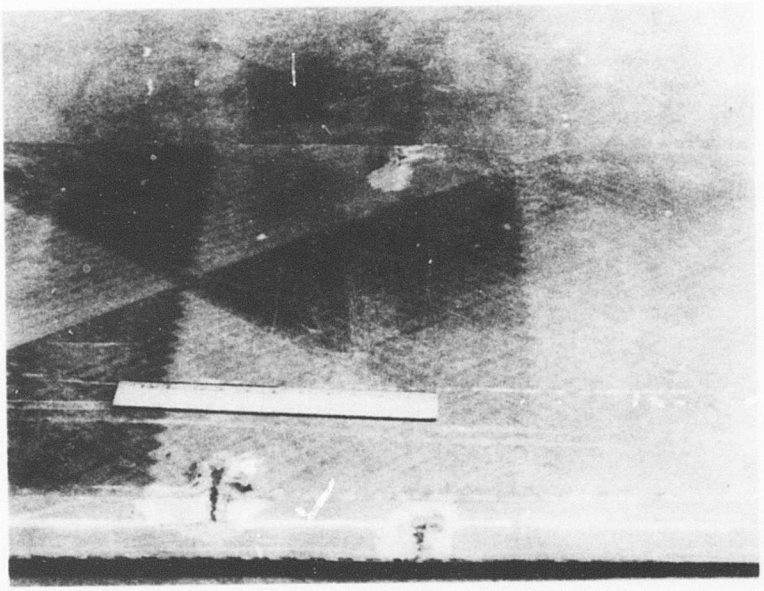

Figure 41. Bullet Damage,
Spar - S/N 003.

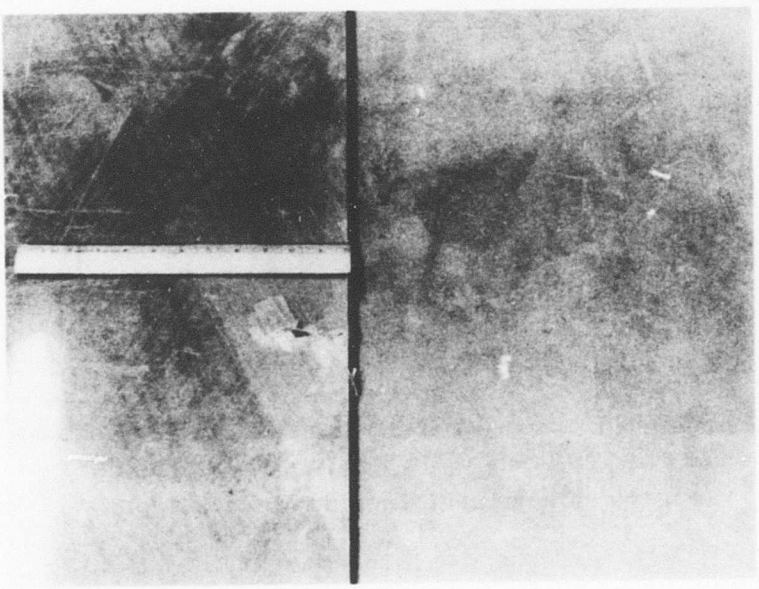

Figure 42. Bullet Damage,
Trailing Edge - S/N 003.

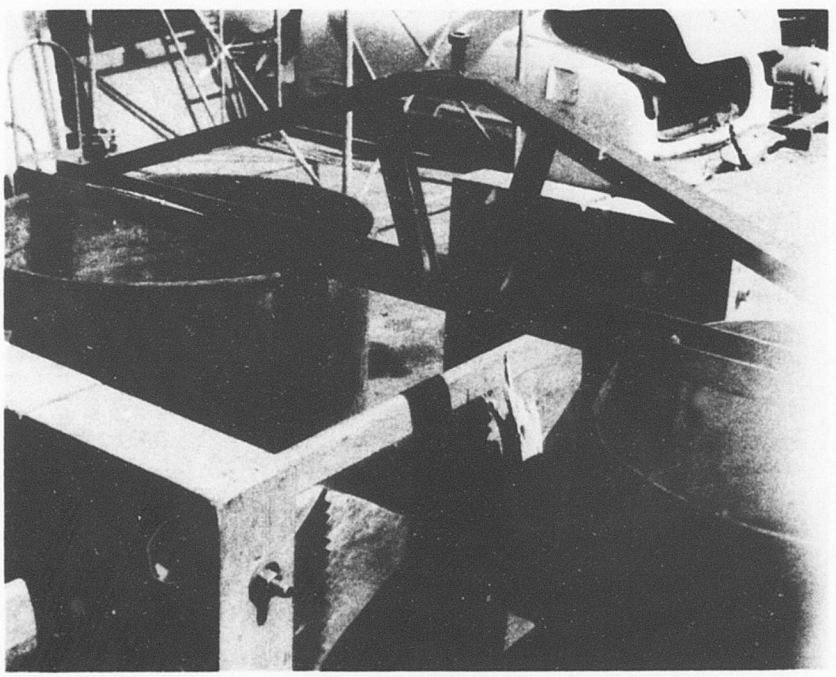

Figure 43. Impact Tree Strike - S/N 003.

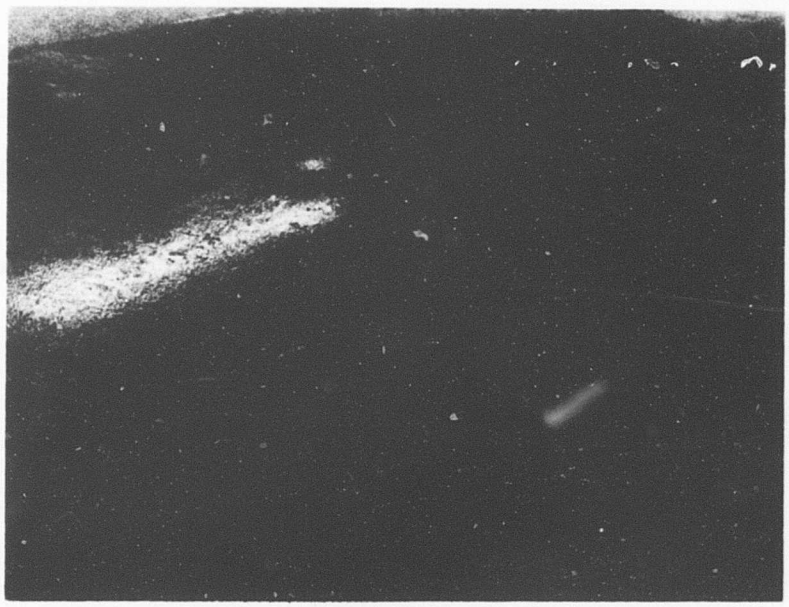

Figure 44. Ball Drop Results - S/N 003.

APPENDIX

BULLET IMPACT REPAIRS

Two blades (S/N-002 and 003) were tested for bullet impact. Only the fiberglass blade, S/N 002, was repaired.

LEADING EDGE REPAIR

Blade Damage

The bullet hit flat on the leading edge of the blade and glanced off into the sand. The damage to the blade was groove shaped, penetrating the skin and gouging out a small area in the surface of the longo material. The groove was approximately 1-1/2 inches long, 1/2 inch wide and 0.30 inch deep. Damage to the skin was approximately 2 inches chordwise and 3 inches spanwise.

Repair Procedure

Repairs were made in the following steps:

1. All damaged material was removed by sanding with an air-operated hand-held rotary disc sander using 60-grit Jewelox paper. At the same time, the sides of the groove in the longo material were tapered out to 3 inches in the spanwise direction. The skin material was then stepped (2 steps, each 1/2 inch wide) past this point.

2. The longo material was replaced using plies of Style 143 fiber glass fabric and a resin system consisting of DOW DER 323 resin and APCO 320 hardener at a ratio of 17.4 parts by weight per hundred. The resin system was applied to each ply of fabric to assure full saturation. The first plies were cut small to fill the bottom of the groove, and each succeeding ply was cut increasingly larger to fill the groove evenly. Twenty plies were required to fill the groove in the longo material.

3. The skin material was replaced using six plies of Style 181 fabric with the fibers placed at an angle of $\pm 45^{\circ}$, and two plies of the same material with the fibers at 0° to the spanwise axis. Again, the same procedure was used of cutting smaller pieces at first and increasing the width and length to fill the hole evenly. The last two plies covered the entire hole, overlapping on each side 1 inch onto the outer surface of the original skin. The same resin system described in Step 2 above was used.

4. Next, the entire repaired area was covered with one ply of Style 113 fabric using the same resin system, and overlapping 2 inches on each side.

5. The entire area was vacuum bagged (28 in. Hg) and cured under heat lamps at a temperature of 200° F for 4 hours.

6. After curing, the vacuum bag was removed, was sanded to remove excess material and formed to the original shape. Progressively finer sanding discs were used to finish the area, beginning with a No. 60 grit air-operated sander and ending with a No. 400 grit hand-held block sander.

7. The entire repair area was then covered with a plastic coating used to restore the natural surface appearance of glass-reinforced plastic structures.

8. The repair required 6 hours including cure time. The cure time was 4 hours.

TRAILING EDGE REPAIR

Blade Damage

The bullet penetrated the trailing edge of the blade and exited on the opposite side, leaving a groove running chordwise for about 1-1/2 inches long at the entrance and about 3 inches long on the exit side. The trailing edge split at the bond line approximately 4 inches on both sides of the bullet entrance. The bullet severed the trailing-edge longo material, and the damage extended forward into the foam area.

Repair Procedure

1. The skin was stripped away on both sides of the blade until the trailing edge longo material and foam were exposed for 7-1/2 inches on both sides of the damaged area and 1 inch in front. The resulting exposed areas were rectangular in shape. Using an air-operated disc sander with No. 60 grit paper, the skin was tapered back 1-1/2 inches on each side of the rectangles.

2. Again, using the sander, the damaged longo material was removed and the two severed ends were sanded to a knife edge taper on the ends with the taper extended back 2 inches on the bullet entrance side and 4 inches on the bullet exit side.

3. Voids in the damaged foam area were filled using a thick mixture of micro-balloons in a resin system composed of DOW DER 332 resin and APCO 320 hardener mixed to a ratio of 17.4 parts by weight per hundred.

4. Four plies of glass cloth Style 181 with fibers running at $\pm$ 45° angles to the trailing edge were first applied to one side of the blade. The first ply was cut to fit the dimensions of the rectangles, and the others were cut progressively 1 inch longer. Each ply was saturated with a resin system consisting of DOW DER 332 resin and APCO 320 hardener mixed at a ratio of 17.4 parts by weight per hundred. Precautions were taken to insure full contact to the tapered portions of the longo material and across the gap at the knife edges.

5. One ply of Style 113 glass was next applied to the side of the blade, using the same resin system used with the 181 glass. The plies were cut to extend over the surface of the original skin 1 inch from the edge of the taper.

6. Forty-six plies of Style 143 glass cloth were applied next to the longo material, using the same resin system used with the Style 181 material. These plies were made by folding a trapezoidal shaped piece cut from the roll with the unidirectional material running across the piece. The piece was 10 inches wide at the base and 17 inches long, with the sides being of equal length. The top leg of the piece installed on the bullet entrance side of the longo material was 2 inches. The fabric was then folded accordion fashion, starting at the top or small side with the first fold approximately 0.04 inch wide and increasing the width of each succeeding ply gradually and equally (ideally in increments of 0.036 inch) until the last and widest fold was 1.5 inches wide. Each ply was placed under the last so that the top side was straight up and down, with the other sides sloped outward in a half-pyramid shape.

   The material when folded in this fashion formed the same shape as the wedge-shaped longo material and at the same time generally fit the contoured sides of the cleaned-out damaged area.

7. Four plies of Style 181 glass cloth were installed over the 46 plies of the Style 143 cloth in the same manner as described in Step 4.

8. One ply of Style 113 cloth was installed over the entire area in the same manner as described in Step 5.

9. The entire area was vacuum bagged (28 in. Hg) and cured under heat lamps at a temperature of 200°F for 4 hours.

10. After curing, the vacuum bag was removed, and the area was sanded to remove excess material and formed to the original shape. Progressively finer sanding discs were used to finish

the area, beginning with No. 60 grit and ending with a No. 400 grit. Air-powered tools were first used, followed by the finish sanding with the No. 400 grit hand-held sander.

11. The entire area was then covered with a plastic coating to restore the natural surface appearance of a glass-reinforced plastic structure.

12. Repair required 4 hours plus another 4 hours for cure.

LIST OF SYMBOLS

A	area (in. ^{2})
AE	spanwise stiffness (lb)
C	coefficient of damping
CG	center of gravity, dist. aft of leading edge (in.)
c	dimension measured from NA (in.)
d	dimension (in.)
E	modulus of elasticity (psi)
EI_x	bending stiffness about x axis (lb-in. ^{2})
EI_y	bending stiffness about y axis (lb-in. ^{2})
F	allowable strength (psi)
G	modulus of rigidity (psi)
I	moment of inertia (in. ^{4})
K	torsional constant (in. ^{4})
KG	torsional stiffness (lb-in. ^{2})
L	length (in.)
M	bending moment (in. -lb)
MS	margin of safety
P	load (lb)
QE	moment area times modulus (lb-in.)
t	thickness (in.)
V	shear (lb), volume ratio
W	weight ratio, unit weight (lb/in.)
x	dimension measured from leading edge (in.)
α	coefficient of thermal expansion (in. /in. /^{o}F), angle (deg)
ϵ	strain (in. /in.)
μ	Poisson's ratio
ρ	density (lb/in. ^{3})
σ	unit stress (psi)
τ	unit shear stress (psi)

Subscripts

b	beamwise direction
bru	bearing ultimate
c	chordwise direction, composite
cu	compression ultimate
r	resin
su	shear ultimate
t	torsion
tu	tension ultimate